AN EXPERIMENTAL INVESTIGATION OF A SAVONIUS WIND TURBINE ROTOR PERFORMANCE FOR LOW WIND SPEED APPLICATIONS

ALICE ACHIENG' KASERA

MASTER OF SCIENCE

(Energy Technology)

JOMO KENYATTA UNIVERSITY OF AGRICULTURE AND TECHNOLOGY

2017

An Experimental Investigation of A Savonius Wind Turbine Rotor Performance for Low Wind Speed Applications

Alice Achieng' Kasera

A Thesis Submitted in Partial Fulfilment for the Degree of Master of Science in Energy Technology in the Jomo Kenyatta University of Agriculture and Technology

2017

DECLARATION

This thesis is my original work and has not been submitted for a degree in any other University.

Signature……..... Date……

Alice Achieng' Kasera

This thesis has been submitted with our approval as University supervisors

Signature:  Date: 31st March, 2017

Mr. Francis Xavier Ochieng,
JKUAT, Kenya

Signature……..... Date……

Prof. Robert Kinyua, PhD.
JKUAT, Kenya

DEDICATION

This work is dedicated to my husband-Mark Ogola and daughter Lainu Mark

ACKNOWLEDGMENTS

This work was financed by the National commission for Science, technology and Innovation under Science, Technology and Innovation (ST & I) – 4TH study grant number: NCST/5/003/4TH STI CALL/037 entitled "Study, Development and standardization of a low cost, locally manufactured small wind pump" whose principal investigator was Mr. Francis Xavier Ochieng' of JKUAT.

My sincere gratitude goes to my supervisors Mr. Francis Ochieng' and Prof. Robert Kinyua both of IEET for their valuable guidance, direction and encouragement throughout the progress of this research. Mr. Njoka of IEET is not forgotten for his continuous advisory role during the research period.

Special thanks goes to Mr. Masinde of mechanical engineering department (JKUAT) for advising me on machining of the stand (base) and the associated mechanical work of rotor blade fitting.

My family is not forgotten for their patience, financial and mental support during this long period of my research. I owe them agape love.

TABLE OF CONTENTS

LIST OF TABLES

LIST OF FIGURES

LIST OF PLATES

LIST OF APPENDICES

LIST OF SYMBOLS

υ_{avg}	Average wind speed
υ	Wind speed
υ_o	Ambient wind speed
ρ	Density=1.224kg/m^3
ω	Angular velocity
σ	Solidity
λ	Tip speed ratio
~	Approximately
<	Lesser than
>	Greater than
≥	Greater than or Equal to

LIST OF ABBREVIATIONS

m/s	Metres per second
P	Power
kg/m^3	kilogram per meter cubed
A	Area (m^2)
m	Metres
Km	Kilometre
E	Efficiency
M	Mass
Cp	Power coefficient
$\mathbf{P_t}$	Theoretical power
P_B	Power of the blade
F	Force
T	Torque
T_B	Torque of the blade
$\mathbf{C_\tau}$	Torque coefficient
H	Height
D	Diameter
R	Radius
C	Chord length
W	Watts
kW	Kilo Watts (10^3 Watts)
HAWT	Horizontal Axis Wind Turbine
VAWT	Vertical Axis Wind Turbine

ASALs	Arid and Semi-Arid Lands
BHEL	Bob Harries Engineering Limited
Rads/s	Radians per second
CFD	Computational Fluid Dynamics
3-D	Three dimension
FEA	Finite Element Analysis
O&M	Operation and maintenance
FRG	Fibre Reinforced Glass
SWERA	Solar and Wind Energy Resource Assessment
BOS	Balance of System
PV	Photo Voltaic
$\mathbf{V_{ac}}$	Alternating current voltage
$\mathbf{V_{dc}}$	Direct current voltage
NACOSTI	National Commission for Science Technology and Innovation
KEBs	Kenya Bureau of Standards
ERC	Energy Regulatory Commission
REA	Rural Electrification Authority
SWOT	Strengths, Weaknesses, Opportunities and Threats.
IEC	International Electro-technical Commissions
WTG	Wind Turbine Generator
RPM	Revolution Per Minute
TSR	Tip Speed Ratio

ABSTRACT

Designing and installation of wind turbine projects globally have boosted power supply to the national grid and other associated works, however, problems associated with the current small scale wind turbines include: High starting wind speed; high capital cost; poor after sales services and maintenance by the suppliers and also collapse of the hub as a result of the structural design. This research focussed on developing Savonius rotor blades using fibre reinforced glass which processes a characteristic of being very light, strong and durable. The generator part was also mounted on the ground which eliminates the collapse of the hub and at the same time easily accessible during maintenance. A field visit to the wind energy market stakeholders was conducted through a questionnaire hence analysis on the strength, weaknesses, opportunities and threats were done. After studying the market, design and development of two models of different power output was done. The models were designed with 2 blades of a semi-circular cross sectional profile, a separation gap of 0.03 m, aspect ratio of 2 and overlap ratio of positive 25%. For the first model upon testing with a direct drive generator, the cut-in-wind speed was found to be at 2.7 m/s which produced a mechanical power of 14.9 N and electrical power of 1.1 W. At the rated wind speed of 7.5 m/s, the power output obtained was 23.32 W instead of the theoretical power of 56.9 W which resulted to a performance (efficiency) of 13%. The second model upon testing, the cut-in- wind speed was found to be below 2.5 m/s since at 2.1 m/s a mechanical power of 11.2 N and electrical power of 242.2 W was obtained at the rated wind speed of 7.5 m/s instead of the theoretical output of 259.9 W which resulted to a performance of 28%.The second prototype was then tested at Ngong' hills (Kajiado county) and it was found that at 1.53 m/s, 0.7 W was obtained. The rated wind speed was not attained on the day of testing but the power output at the highest measured wind speed of 6.44 m/s was 228.2 W which resulted to a performance of 44%.The above results led to a conclusion that it is possible to locally develop a wind turbine rotor blades (in a local workshop with locally available tools and materials), that is more efficient and adaptable for Kenya's average wind speed of 4 m/s.

CHAPTER ONE

INTRODUCTION

1.1 Background

Global climatic changes have been a direct effect of environmental pollution due to excessive use of fossil fuel. This calls for use of clean renewable energy in day to day activities to safeguard the flora and fauna. The concept of harnessing wind energy has been overwhelmingly embraced all over the world. Ali (2013) further explained that vertical axis wind turbines provide a more reliable energy conversion technology as compared to horizontal axis wind turbines, especially in areas of lowly rated and/or uncertain wind speeds.

There are two types of wind turbines: Horizontal Axis Wind Turbine (HAWT) and Vertical Axis Wind Turbine (VAWT). A study conducted by Mathew (2006) showed that HAWTs are the most commonly known types of wind turbines which operate parallel to the direction of the wind whereas VAWTs rotors operate perpendicular to the direction of wind. Even though HAWTs have proved to be effective in other developed countries, they possess some problems and disadvantages like: Higher starting wind speed ($\geq$ 3 m/s), require stable wind direction, encounter turbulence which reduces efficiency, the power stability changes with wind direction, are very noisy ~45 dB or more, require high installation height to avoid the terrain turbulence and must therefore be installed in open areas, however, they have a high energy conversion performance.

On the other hand, VAWTs have so many advantages which include: Low starting wind speed of as low as 1-2 m/s, effective at any wind direction and the efficiency is not affected with turbulence hence stable power is achieved without any wind direction effect, not noisy, installation height is low (not affected by turbulence), the generator and gearing system is always mounted at the base which makes the whole system easier to access during maintenance and / breakdown, any location is recommended for

installation and does not require a wide area, however they have a low energy conversion performance hence calls for a research on design and development of a higher performance Savonius wind turbine rotor blade.

Designing and installation of wind turbine projects globally have boosted power supply to the national grid and other associated works, however, under conditions of low wind speeds, HAWTs do not perform so well compared to VAWTs as found by Mathew (2006). A locally manufactured VAWT would perform amicably in these conditions considering the installation, operation and maintenance cost. Commercially available wind turbines are currently picking up in Kenya following the installation currently in Ngong' (Kajiado County) currently producing 5.1 MW, Turkana (Turkana County) to produce 310 MW and Meru (Meru County) to produce 400 MW upon completion. (www.kengen.co.ke). However these types of wind turbines usually amount to high installation costs with a long payback period. They also require a lot of space as well as expertise for such applications. To utilize the available wind resources at whatever height, small scale wind turbines are therefore recommended for use at homes, street lightings, institutions like churches, schools, among others.

From the local market survey, the available small scale wind turbines ($\leq$ 3 kW) installed by a few individuals were found to be very expensive ranging between Kshs. 250,000 and 1 million depending on the turbines' rating and or customers' demand. This research was to design and fabricate a cheaper and a higher performing small scale wind turbine rotor blade using the local available materials for an output of 250 W for mechanical and/ or electrical applications.

1.2 Problem Statement.

The general problems with the current installed small scale wind turbines include: High starting wind speed; high capital cost which makes it less attractive for persons or communities with less economic power; poor after sales services and maintenance by

the suppliers which results to the broken and worn out rotor blades; corrosion of the blades due to the materials used (aluminium alloy) and collapse of the hub as a result of the structural design i.e. the gearbox and the generator are mounted at the top causing imbalance during windy or stormy seasons.

The research focussed on developing a Savonius rotor blade using local available materials which would eventually lower the cost. This type of wind turbine has the hub placed on the ground which makes it easier to maintain and at the same time totally eliminates the possible collapse of the hub during windy stormy seasons. The rotor blades were also made from Fibre Reinforced Glass (FRG) which is very light (makes the blade start rotating at a very small wind speed of less than 3 m/s), strong, does not rust and durable and any shape can easily be obtained from the fibre mould.

1.3 Justification of the Study

The rotor is that component of a wind turbine which converts the flow of an air mass into mechanical rotational energy. Therefore, this component and its interfaces with other components are of utmost importance. Its fabrication and utilization depends on the prevalent wind speeds at the site of installation, its costs and also quality of manufacture.

For small domestic applications in low wind speed areas, the use of a low cost, highly performance wind turbine that can operate in a low wind regime of less than 5 m/s would be desirable. Unfortunately, the locally available wind turbines are very inefficient and the imported ones are very expensive with a lot of imported expertise involved. All these factors combined make a complete turbine quite unaffordable to most communities or individuals with less economic power as explained by Harries (2002).

1.4 Hypothesis

It is not possible to develop Savonius VAWTs rotor blades of higher performance than the conventional wind turbines. Using the locally available materials, locally manufactured Savonius rotor blades would cost more than the conventional varieties in Kenya.

1.5 Objectives

1.5.1 Main Objective

To experimentally investigate a Savonius wind turbine rotor performance for low wind speed applications.

1.5.2 Specific Objectives

1. To analyse the Strengths, Weaknesses, Opportunities and Threats (SWOT) in the local wind energy market.
2. To design, fabricate and characterize Savonius rotor blades for low wind speed applications.
3. To assess (analyse) the cost of production and operation of the fabricated Savonius rotor with respect to conventional wind turbines.

1.6 Scope of the Study

This research was limited to Savonius rotor blade manufactured using fibre reinforced glass for applications in areas with low wind speeds. The whole process began from a survey from the local market where most of the important and reliable information was obtained, there after design of the rotor blades was done using theoretical calculated formulae. Prototypes of different power output were fabricated in a laboratory and testing separately using a fabricated industrial fan as the air source to study the aerodynamic characteristics of the blades.

Measurements of different parameters were done using the measurement instruments i.e. an anemometer for wind speed, tachometer for torque, an ammeter and voltmeter for current and voltage respectively. The output power was analyzed using power analyser and monitored using a cathode ray oscilloscope.

Safety of any type of wind turbine depends on the power regulation strategy. It is an important issue at high wind speeds to ensure that loads do not reach their maximum admissible values however due to the limited time and finances, it is out of the scope of this study to include control strategy in the design process.

1.7 Study Limitations

The design of the rotor blade was done to the JKUAT's average wind speed which was found to be 5 m/s from a research conducted by Saoke *et al.* (2011). However, some field tests were done outside Juja which had different average wind speed, thereby generating a different power curve from the expected design power curve. This type of wind turbine and especially VAWTs are not locally manufactured in Kenya. Comparison was therefore done with the imported ones and the conventional HAWTs.

CHAPTER TWO

LITERATURE REVIEW

2.1 Theory of Historical and Modern VAWTs Rotor Designs

The configuration for the shaft and rotor orientation of this type of turbine according to Schubel and Crossley (2012) is that the rotor shaft is perpendicular to the ground as shown in figure 2.1. Ali (2013) also found that they are unpopular especially in developing countries and its transmission system is mounted at the bottom of the rotor shaft.

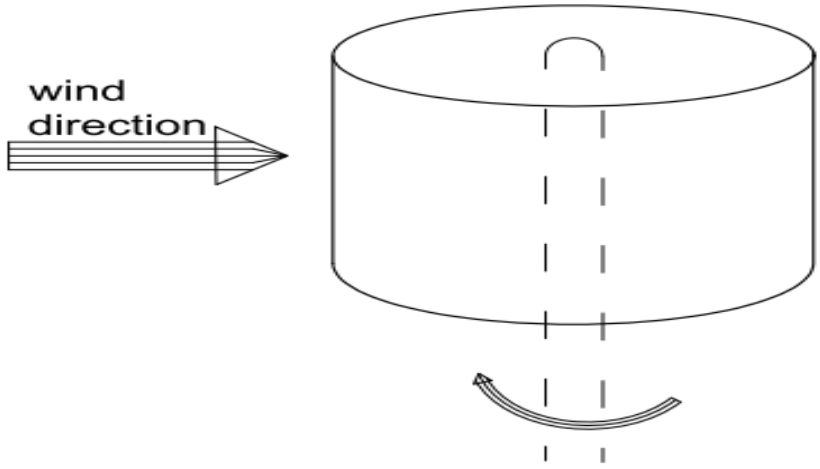

Figure 2.1: Rotor and shaft orientation of VAWTs. (Schubel & Crossley, 2012)

2.1.1 The Persian Windmill

The earliest documented wind mill was produced in 900 A.D by an ancient Persian for grinding grains. This type of wind mill had a vertical axis and force was derived by

means of the aerodynamic drag generated by flat plates in the wind as shown in Table 2.1. These windmills were however very big approximately measuring 5 m long and 9 m tall. By the 12th century, these types of wind mills were very popular in Europe, France by 1105 A.D and England by 1191 A.D as narrated by Schubel and Crossley (2012) as well as Mathew (2006).

Table 2.1: Summary of the historical and modern vertical rotor blades. (Peter & Richard, 2012)

Design	Orientation	Application	Max. Efficiency	Diagram
Savonius rotor	VAWT	Historic Persian wind mill to modern day ventilation	16%	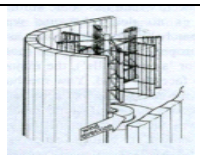 Persian  (b) Modern Savonius rotor
Darrieus	VAWT	20th century for generating electricity	40%	 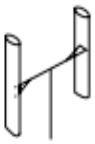
Hybrid	VAWT	Electricity production	55%	 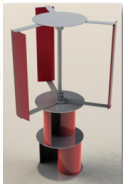 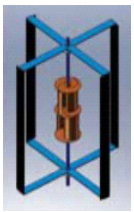

2.1.2 Savonius Wind Turbine.

The first Savonius wind turbine was invented by S.J. Savonius as a drag type machine in the late 1920s. Savonius turbines are basically drag machines which typically have rounded paddles that catch wind in the cap and shed it on the rounded fronts allowing the difference in drag to rotate the turbine. The earlier type of this VAWT machine involved cutting a cylinder into two halves along the central plane and then moving the two half cylinders sideways along the cutting plane so that the cross-section resembled the letter 'S' shape as explained by Mathew (2006). Since then a lot of engineering calculations like overlap ratio, tip speed ratio, aspect ratio, separation gap among others are being considered for maximum performance.

2.1.2.1 Principle Operation of a Savonius Rotor

The Savonius rotor works due to the difference in forces exerted on each blade. At any position there must be an advancing blade (concave half to the wind direction) that catches the wind and forces the blade to rotate around its central vertical shaft. On the other hand, the retreating or returning blade (Convex half to the wind direction) hits the blade and causes the wind to be deflected sideways around it. Because of the blades curvature, the blades experiences less drag force when moving against the wind than the blades when moving with the wind. Hence the advancing blade with concave side facing the wind experiences more drag force than the retreating or returning blade, thus forcing the rotor to rotate as illustrated in figure 2.2 and 2.3.

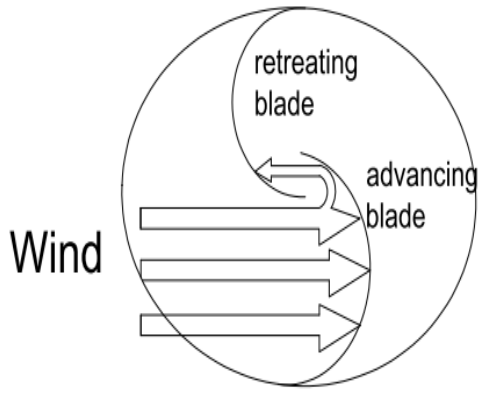

Figure 2.2: Principle operation of Savonius rotor.

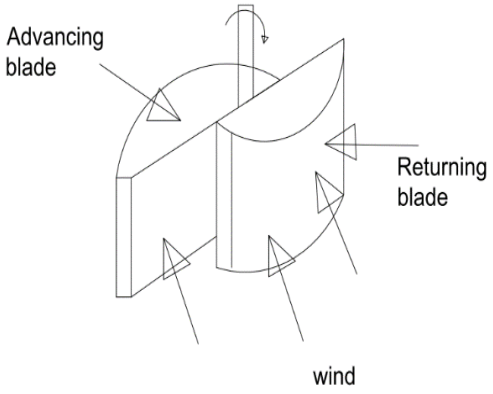

Figure 2.3: A 3-D conventional view of a Savonius rotor.

The Differential drag causes the Savonius turbine to spin as explained by Mathew (2006) and Ali (2013). Zingman (2007) also explained how a lot of research has been done on the Savonius wind turbine which proved to have a low tip speed ratio with a high solidity creating a high torque suitable for pumping water.

2.2 Previous Work Relevant to the Study

Emmanuel *et al*. (2011) conducted an experiment in order to improve the performance of Savonius turbines by increasing the number of blades and by preventing the wind from impinging on the convex parts. They found that shielding the rotors can achieve higher performance and at the same time having a six bladed rotor can achieve power coefficient performance of around 0.3.

Ali *et al*. (2012) studied the performance of Savonius turbine by incorporating a flow restricting cowl and testing different types of configurations. They found that the fully cowled configuration had the least performance and produced rotation only for high rotation speeds. However the partially cowled configuration gave a better performance for both centred and closed conditions. It was also observed that the closed position reduced the resistance and increased the rotational motion.

Mohammed *et al.* (2010) conducted experiments on Savonius rotor by attaching half cylinder disks on the central rotor. This work focussed mainly on the concept of obstacle plate at the optimum configuration in order to increase the efficiency and utilize mainly as an energy source for commercial purposes. It was found that this type of turbine with all the considerations was only effective for domestic purposes.

Damak *et al.* (2012) conducted experiments on a helical Savonius rotor with a twist of 180^0. The aerodynamic study of the helical Savonius and the effect of Reynold's number and overlap ratio on the performance of the helical Savonius rotor were also studied. It was found that the rotor with the helical geometry yields better performance characteristics and was very sensitive to the change in the Reynold's number than that of the conventional one.

Kolachana (2012) did an analysis after designing a Savonius wind turbine by using a computer model rather than experimental model but found out that the experimental study results were limited to the design being tested since when a particular input was

changed then the change in the output was not readily available unless sensitivity information was available. In as much as the computer models provided the user with the privilege to change inputs and see the outcome instantly, however, the computer models were only approximations of the experiments and were also limited in modelling the actual physics.

Widodo *et al.* (2012) designed a Savonius rotor blade to generate 5 kW power output. The rotor diameter was 3.5 m with a height of 7 m. The 3D model was created using Solid work software. Computational Fluid Dynamic (CFD) was performed to obtain pressure difference between concave and convex region of the blade and Finite Element Analysis (FEA) was done to obtain the structural response of the blade due to the wind load applied. The group had difficulties from the software and the computer capability i.e. in real world scenario, when the air flows through the blade, it could induce a force to turn the rotor blade, however, the solid works software was unable to perform the CFD analysis while the blades were turning (dynamic situation) hence only the static CFD was performed.

Kamoji *et al.* (2009) did an experimental investigation on single stage modified Savonius rotor to improve the power coefficient and to obtain uniform static torque coefficient. These were achieved by studying the rotor with and without the central shaft between the end plates. The Savonius rotor with central shaft was tested in a closed jet wind tunnel and a power coefficient of 0.32 was obtained. The modified Savonius rotor without the central shaft was tested in an open jet wind tunnel. Investigation was undertaken to study the effect of geometrical parameters on the performance of the rotors in terms of static torque coefficient, torque coefficient and power coefficient. Results concluded that the modified (without central shaft) Savonius rotor with an overlap ratio of 0, a blade arc angle of 124^0 and an aspect ratio of 0.7 resulted in a maximum power coefficient of 0.21 which was higher than that of conventional Savonius rotor of 0.19.

Altan *et al.* (2008) did a study by introducing a curtaining arrangement to improve the performance of Savonius wind rotors. The curtain arrangement was placed in front of the rotor to prevent the negative torque opposing the rotor rotation. The geometrical parameters of the curtain arrangement were optimized to generate an optimum performance. The rotor with different curtain arrangement was tested out of a wind tunnel, and its performance was compared with that of the conventional rotor. The maximum power coefficient of the Savonius wind rotor was increased to about 38.5% with the optimum curtain arrangement. The experimental results showed that the performance of Savonius wind rotors could be improved with a suitable curtain arrangement.

Saha *et al.* (2008) conducted wind tunnel tests on 84 different prototypes of Savonius rotor models of the same dimension, same number of blades (two and three), stages (single and double) and geometry (semi-circular and twisted). Further attempts were also done to investigate the performance of two stage rotor system by inserting valves on the concave side of the blade by maintaining the wind speed at between 6 m/s and 11 m/s. Amongst the 84 experiments done they found that the two-bladed double-stage Savonius model showed the highest value of power coefficient. The twisted model was found to have more performance than the semi-circular to approximately 27% however it was very expensive, and difficult to design and construct.

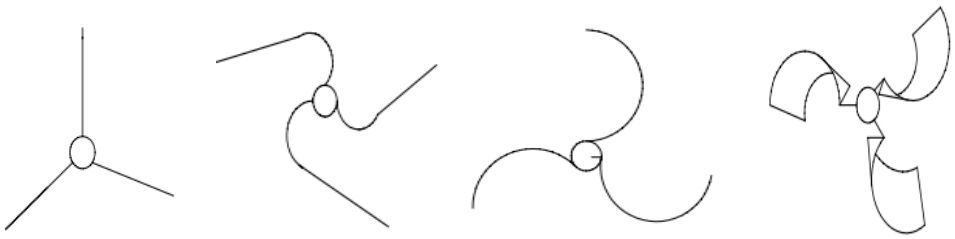

(i) Straight (ii) Aerofoil (iii) Curved (iv) Twisted

Figure 2.4: Different blade designs (i-iv) tested by Saha *et al.* (2008).

Sheldahal *et al.* (1978) performed experiments of a new type of helical bladed Savonius rotor and compared the results with the conventional Savonius rotor. They found that the optimum rotor power coefficient was 0.2 for a two bladed rotor at a height to diameter ratio of 6.

Previous published research show that most of the successful experiments had lower performance of < 30%. Other research with higher performance of ≥ 30% had a drawback of being very expensive. The rest which achieved performance of ≥ 40% were quite impractical experimentally. Therefore the present study capitalized on the aspect of design which would have higher performance of ≥ 30%, practicable, cheap and easy to construct for low wind speed applications.

2.3 Regulatory Framework.

Review of relevant government documents was done to determine whether there are policies and instruments that support the development of small wind energy market in Kenya. The reviewed documents were:

2.3.1 Sessional paper No.4 on Energy, (2004) (6.4) (1).

This document enhances the government through the Ministry of Energy to formulate and enforce standards and codes of practice on renewable technologies to safeguard consumer interests, Promotes research in development and demonstration of the manufacture of cost effective renewable energy technologies (the researcher is a beneficiary of this funding from the National Council for Science Technology and Innovation-NACOSTI). It promotes development of appropriate local capacity for manufacture, installation, maintenance and operation of basic renewable technologies, promotes development and widespread utilization for renewable energy technologies which are yet to reach commercialization and allows duty free importation of renewable energy hardware. The Energy bill, 2015 (90) (2) and The Energy Act, 2006 also promotes research and development in different capacities.

2.3.2 Kenya Bureau of Standards:

This organization develops standards and codes of practices. The available International standards for small wind turbines are: IEC 61400-2: 2013 for Safety philosophy, Quality assurance, and engineering integrity, i.e. design, installation, maintenance and operation, IEC 61400-23:2014: Defines the requirements for full scale structural testing of wind turbine blades: Static load, fatigue, static load tests after fatigue and other blade properties.

2.4 Theoretical Calculations

This involves all the parameters considered in the rotor blade design which included: Wind speed, Power and power coefficient, Torque and torque coefficient, Swept area, Tip speed ratio, Solidity, Number of blades, Aspect ratio, Overlap ratio, and Separation gap.

2.4.1 Wind Speed

This is the major element that affects the power output. The three wind speed parameters that were used in this project were: Cut-in wind speed, rated wind speed and cut-out wind speed, which are related to the power performance as stated by Jain (2011) and applied by Widodo *et Al.* (2012) to design and analyse a 5 kW Savonius rotor blade.

$$\mathbf{V_{cut\text{-}in} = 0.5\ V_{avg}} \qquad \mathbf{(2.1)}$$

When the turbine starts to produce power. V_{avg} is the average speed/ velocity of the wind which is 5 m/s in Juja according to the study conducted by Saoke *et al.* (2011). Therefore,

$$V_{cut\text{-}in} = 0.5 \times 5 = 2.5 \text{ m/s}$$

$$\mathbf{V_{Rated} = 1.5\ V_{avg}} \qquad \mathbf{(2.2)}$$

When the turbine reaches its maximum output power.

$$= 1.5 \times \mathbf{5} = 7.5 \text{ m/s}$$

$$\mathbf{Vcut\text{-}out = 3.0\ V_{avg}} \qquad \mathbf{(2.3)}$$

When the turbine cuts out its further production to prevent damage at higher speeds.

$$V_{cut\text{-}out} = 3.0 \times \mathbf{5} = 15 \text{ m/s}$$

2.4.2 Power

The power of the wind is proportional to the mass of air (air density), amount of air (area of the segment of wind) being considered and the speed of air (natural wind speed). Equation 2.4 gives the relationship as explained by Mathew (2006) and Manwel *et al.* (2009).

$$\boldsymbol{P_w = 0.5 \times \rho \times A \times V^3} \qquad \mathbf{(2.4)}$$

Where, P_w is the power of the wind (W), ρ is the air density (kg/m^3), A is the area of the segment of the wind being considered (m^2) and υ is the undisturbed wind speed (m/s).

Manwel *et al.* (2009) further explains that equation (2.4) is the theoretical power i.e. not all the 100% power can be extracted by the turbine since some of the energy may be lost in gearbox, bearings, generator transmission and pressure changes across the turbine blades, hence a constant of $^{16}/_{27} = 0.593 = 59\%$ known as the Lanchester-Betz limit or power coefficient is considered i.e. 59.3% of the power in the wind can be extracted in the case of an ideal turbine. Hence, equation (2.4) becomes

$$P_B = {}^1/_2 \times C_p \times \rho \times A \times V^3 \qquad (2.5)$$

$$P_B = {}^1/_2 \times \rho({}^{16}/_{27} \times A \times V^3)$$

For an ideal wind turbine; $P_B = 0.3 \times \rho \times A \times V^3$, **(2.6)**

According to Jain (2011), the maximum power coefficient, C_p for Savonius rotor is 0.30. Hence the C_p value used in this research is 0.30 and the power output, P_B with consideration of power performance, equation (2.5) therefore becomes;

$$P_B = {}^1/_2 \times \rho(0.3 \times A \times V^3)$$

$$= 0.15 \times \rho \times A \times V^3 \qquad (2.7)$$

Peter & Richard (2012) stated that power of the turbine (P_B) can also be obtained by measuring the Revolution Per Minute (RPM) and the torque of the rotor using tachometer and torque meter respectively and is related as;

$$P_B = ({}^{RPM}/_{60}) \times \text{Torque} \qquad (2.8)$$

2.4.3 Torque

Torque is mathematically defined as the product of magnitude of force and the perpendicular distance of the line of action of the force from the axis of rotation. (Nelkon & Parker, 1995)

$$T = F \times R \qquad (2.9)$$

However, the thrust force (F) experienced by a rotor torque is expressed by Mathew (2006) as

$$F = 0.5 \times \rho_a \times A_T \times V^2 \qquad (2.10)$$

Therefore the rotor torque which is the maximum theoretical torque then becomes

$$T = 0.5 \times \rho_a \times A_T \times V^2 \times R \qquad (2.11)$$

where R is the rotor diameter. (Mathew, 2006).

By inserting the density, area, wind speed and rotor diameter values then equation (2.15) yields, i.e. ρ_a =1.224 kg/m^3, A_T= 3.2 m^2, wind speed = 7.5 m/s and D = 1.3 m then theoretical torque T_{th} becomes 143.2 NM for the 250 W power output.

From equation (2.8), Torque can also be expressed as

$$Torque = \frac{60 \times P_B}{RPM} \qquad (2.12)$$

2.4.4 Power coefficient and Torque coefficient

Power Coefficient (Cp) is a ratio of power of the turbine to the power of the wind and is mathematically presented as:

$$Cp = \frac{Power\ of\ the\ turbine}{Power\ of\ the\ wind} = \frac{P_B}{P_w} \qquad (2.13)$$

Coefficient of power (Cp) obtained from aerofoil empirical curves remains ≃ 0.4 - 0.45 for HAWTs and 0.3 for VAWTs as stated by Manwel *et al.* (2009) and Jain (2011). Widodo *et al.* (2012) in his research also found that the Cp value for Savonius rotor stands at 0.30 and used his findings to design and analyse a 5 kW Savonius rotor blade.

From Wekesa *et al.* (2016), Cp can be defined as

$$Cp = \frac{P_B}{P_W} = \frac{T_B W}{\frac{1}{2}\rho A V^3} = \frac{T_B}{\frac{1}{2}\rho A V^2 R}\frac{\omega R}{V} = C_T \times \lambda, \qquad (2.14)$$

Where T_B is the turbine blade torque, λ is is the tip speed ratio, and C_T is torque coefficient, also expressed by Mathew (2006) as the ratio between the actual torque developed by the rotor and the theoretical torque.

$$C_T = (2T_T) \div (\rho_a \times A_T \times V^2 \times R) \qquad (2.15)$$

Wekesa *et al.* (2016) also described the torque coefficient as the ratio between the actual turbine rotor blades and the theoretical torque, given as,

$$C_T = \frac{T_B}{\frac{1}{2}\rho A V^2 R} \qquad (2.16)$$

2.4.5 Swept Area

Swept area (A) for a VAWT depends on both the turbine's diameter and the turbine's blade length as described by Mathew (2006). Hayashi *et al.* (2004) also found out that the swept area of a Savonius wind turbine is a product of the rotor's diameter and the height, i.e.

$$A = D \times H \qquad (2.17)$$

Johnson (1998) suggested that Savonius rotor performs better when designed with rotor height twice of rotor diameter which leads to better stability with proper efficiencies. Hence,

$$H = 2D \qquad (2.18)$$

by inserting equation (2.18) into equation (2.17) yields,

$$A = 2D^2 \qquad \textbf{(2.19)}$$

In this study, for a power output of 250W and by substituting P_B with 250W, density= 1.224 kg/m^3 and wind speed of 7.5 m/s in equation (2.7), then area (A) becomes:

$$A = \frac{P_B}{0.15 \times \rho \times V^3} \qquad \textbf{(2.20)}$$

$$A = \frac{250}{0.15 \times 1.224 \times 7.5^3} = 3.23\text{m}^2. \cong 3.2\ m^2$$

Since A= 3.2 m^2, substituting this value in equation (2.19) where $A = 2D^2$ then

Diameter (D) = $\sqrt{\frac{A}{2}}$ = 1.3 m hence radius becomes 0.65 m. Substituting the diameter value in equation (2.18) yields, $H = 2D = 2 \times 1.3 = 2.6\ m$.

Figure 2.5 illustrates the above mentioned parameters of the diameter (D) and height (H).

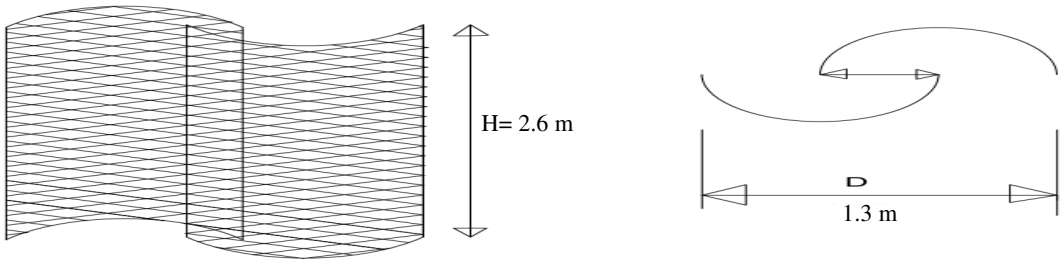

Figure 2.5: Height and diameter dimensions for the 250 W designed rotor blade.

2.4.6 Tip speed ratio (λ)

Mathew (2006) defined Tip Speed Ratio (TSR) as the ratio between the tangential speed at blade tip and the actual wind speed mathematically expressed as,

$$TSR = \frac{Tangential\ speed\ at\ the\ blade\ tip}{Actual\ wind\ speed} \qquad (2.21)$$

Paraschivoiu (2002) and Wekesa *et al.* (2016) in equation (2.14) also explained TSR as the ratio of power coefficient to torque coefficient. Combining the two explanations gives

$$\frac{C_P}{C_T} = \frac{R\omega}{V_0} = \lambda \qquad (2.21)$$

Where ω is the angular speed (rad/s), R the rotor diameter (m) and v_0 the ambient wind speed (m/s). Zingman (2007) also stated that there is an inverse relationship of the TSR and the number of blades, i.e. the higher the TSR the lower the blades and a summarised table given by Zingman (2007) is shown in Table 2.2.

Table 2.2: Tip speed ratio verses number of blades. (Zingman, 2007)

TSR	No of Blades
1	8-24
2	6-12
3	3-6
4	3-4
>4	1-3

A two-bladed Savonius rotor blade was chosen hence the TSR must be >4.

2.4.7 Number of Blades

Saha *et al.* (2008), Zhao (2009) and Ali (2013) supported through an experimental investigation that the two-bladed Savonius rotor has higher performance than three-bladed Savonius rotor because increasing the number of blades increases the drag surfaces against the wind air flow hence increases the reverse torque and eventually reduces the net torque working on the blades. Raghed (2014) also studied the effect of number of blades on the TSR and proved mathematically that the smaller the number of blades, the faster the wind turbine rotates hence extract maximum power from the wind, i.e. for an n bladed machine, s is equal to about half the rotor radius

$$s = \frac{1}{2}\,\mathrm{r}$$

$$\frac{s}{r} = \frac{1}{2} = 0.5$$

$$\lambda_{opt} = \frac{2\pi}{n}\frac{r}{s} = \frac{4\pi}{n} \qquad (2.22)$$

When $n = 2$, then $\lambda_{opt=}$ 6.28, and 4.19 when $n = 3$ etc. This implies that the TSR reduces as the number of blades increases hence reduces the rotor performance. A two-bladed rotor was therefore chosen for this project.

2.4.8 Solidity (σ)

This is the ratio of total rotor area to the total swept area. It affects self-starting capabilities and is determined when the assumptions of the momentum models are applicable, and only when using σ of ≥ 0.4 a self-starting turbine is achieved according to Zingman (2007).

Kumar & Prashant (n.d) mathematically expressed solidity as:

$$\sigma = \frac{N \times A}{\pi R^2} \qquad (2.23)$$

where N is the number of blades, C is the blade chord length (m), R is the wind turbine radius (m).

Practical action (www.practicalaction.org) in their technical brief also defined Solidity as the percentage of the circumference of the rotor which contains material rather than air. They further explained that high- solidity machines carry a lot of material hence generate higher starting torque but with a lower performance than low- solidity machines. A summary of the rotor characteristics given by the Practical action-Technical brief is shown in table 2.3.

Table 2.3: Comparison of rotor types characteristics (www.practicalaction.org)

Type	Speed	Torque	Manufacture	C_P	Solidity (%)
Horizontal Axis					
Cretan Sail	Low	Medium	Simple	0.05-0.15	50
Cambered Plate fan	Low	High	Moderate	0.15-0.30	50-80
Moderate speed aerogenerator	Moderate	Low	Moderate	0.20-0.35	5-10
High speed aerogenerator	high	Very low	Precise	0.30-0.45	< 5
Vertical Axis					
Panemone	Low	Medium	Crude	>0.10	50
Savonius	Moderate	Medium		0.15	100
Darrieus	Moderate	Very low	Precise	0.25-0.35	10-20
Variable geometry	Moderate	Very low	Precise	0.20-0.35	15-40

2.4.9 Aspect Ratio

This is the ratio of the rotor height to the width. However a large aspect ratio of 2-3 provides the rotor with good torque and higher stability as explained by Modi & Fernando (1989) and Johnson (1998). An aspect ratio of 2 was chosen for this research.

$$\textbf{Aspect ratio} = H/C \qquad \textbf{(2.24).}$$

where, H is height of rotor and C is width of rotor (chord length).

2.4.10 Overlap Ratio

This is the ratio of the diameter of the rotor blade to the distance which the blades overlap. For buckets of semi-circular cross-section, the appropriate overlap ratio is 20% to 30% according to Modi & Fernando (1989). A positive 25% overlap ratio was chosen for this research.

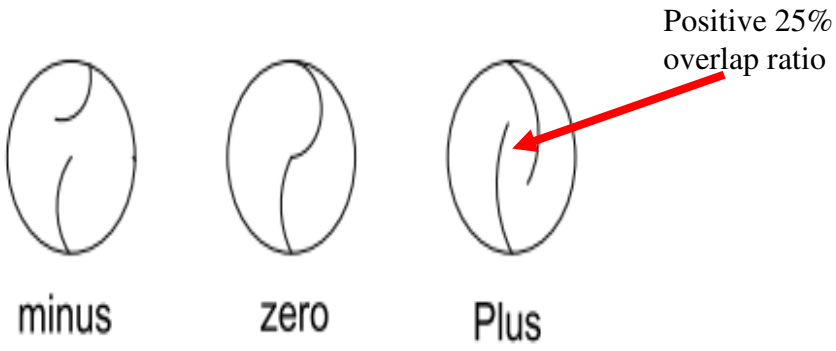

Figure 2.6: Overlap ratio. (Modi & Fernando, 1989)

2.4.11 Separation Gap

This is the distance of the rotor blades from the vertical axis. An increase in the separation gap ratio results in a decrease in the torque coefficient and the power coefficient (Modi & Fernando, 1989). A small negative gap of 0.03 m was used. This

gap equalled to the diameter of the rotor shaft used. ($b = 0.03\ m$)

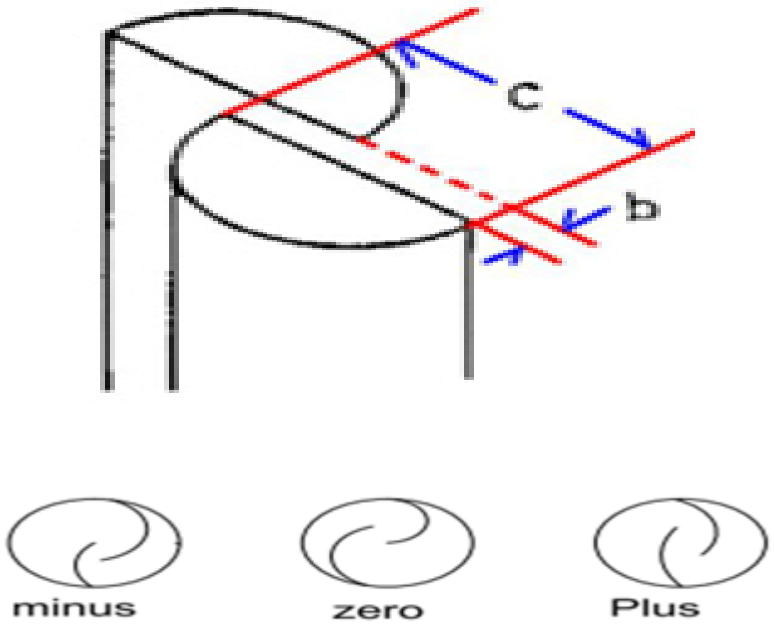

Figure 2.7: Separation gap (Modi & Fernando, 1989)

2.4.12 Cross Sectional Profile

There are two types i.e. Semi-circular and Batch type as explained by Albani & Ibrahim (2013) and is illustrated in Figure 2.8 and Figure 2.9. The number of stages of rotor equals the number of levels of rotor. For this design, the semi-circular single stage type was chosen, even though a double-stage rotor was found to be slightly superior to the corresponding single-stage rotor in both torque and power output as per the research conducted by Albani & Ibrahim (2013).

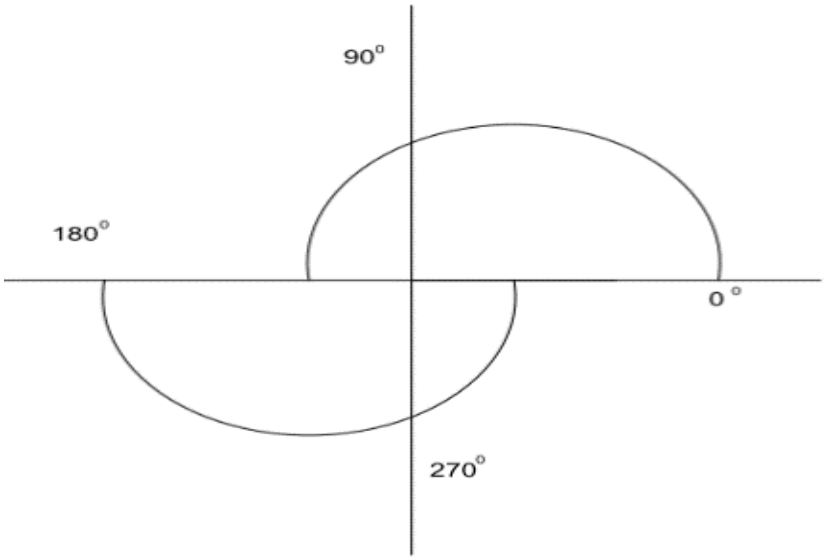

Figure 2.8: Semi-circular (Albani & Ibrahim, 2013)

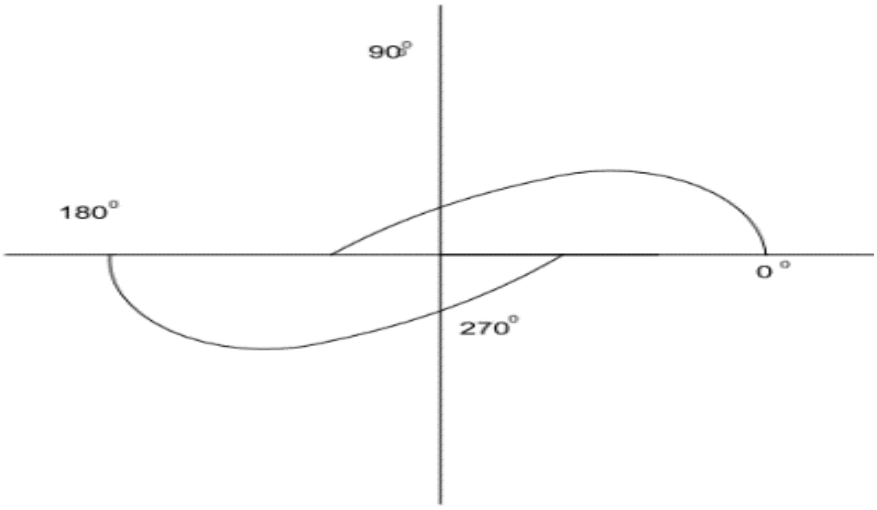

Figure 2.9: Batch type (Albani & Ibrahim, 2013)

2.5 Theoretical Characteristics of Wind Rotor Performance.

The rotor performance is characterized by the efficiency with which the rotor can extract power from the wind which depends on the dynamic matching between the rotor and the wind. These characteristics are represented by the power coefficient and the TSR relationship. This relationship describes the rotor performance irrespective of the rotor size and site parameters as shown in Figure 2.10.

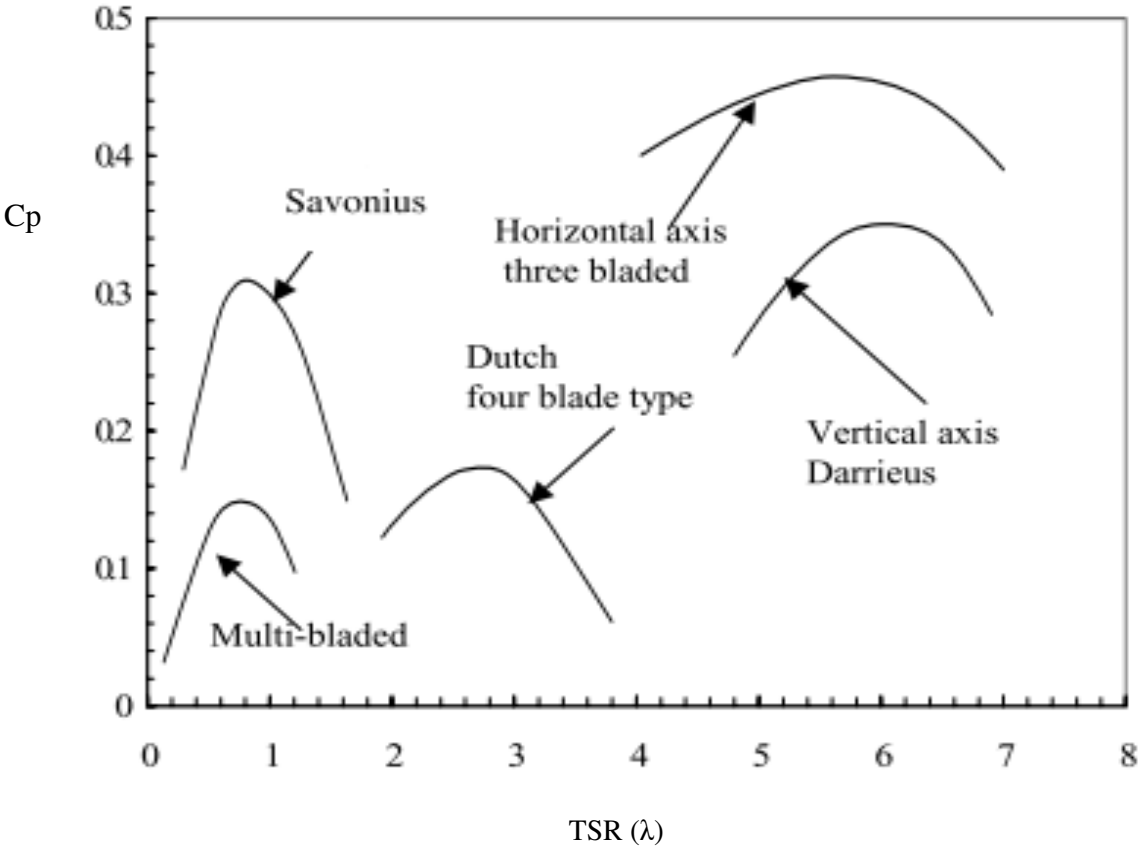

Figure 2.10: Typical rotor performance characteristics for different rotor blades (Peter & Richard, 2012)

Rotor characteristic curves from the previous research are also shown in Figure 2.11 and Figure 2.12.

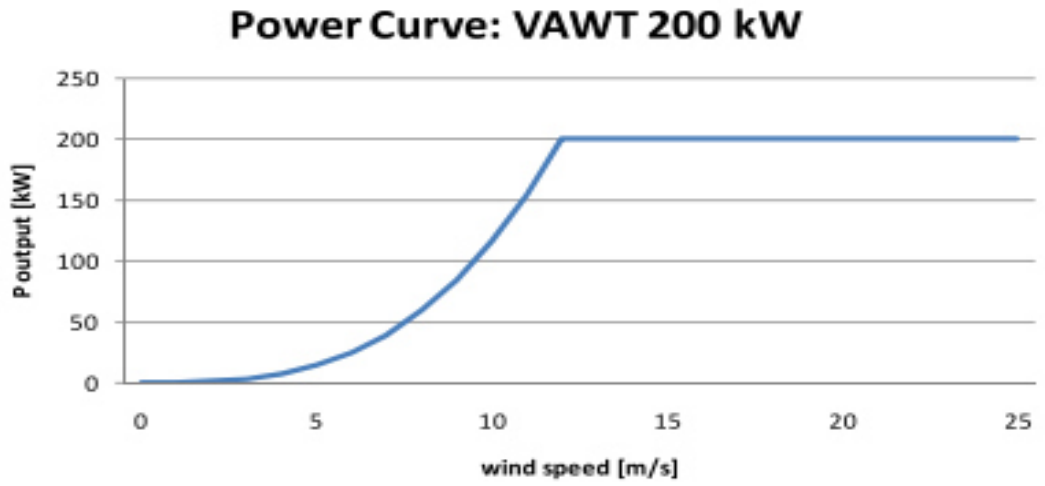

Figure 2.11: Power curve of 200 kW VAWT of power output Falkenberg. (www.wind- power- program.com)

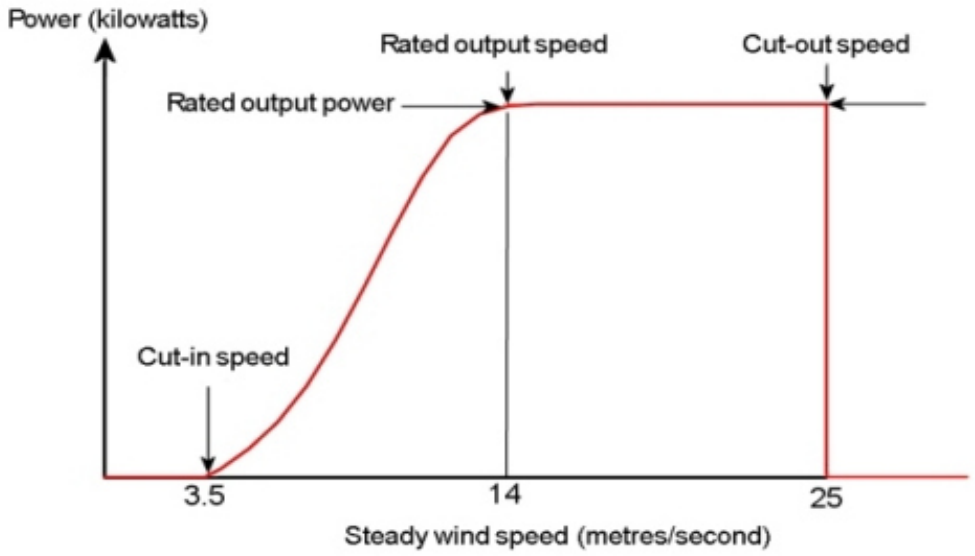

Figure 2.12: Typical wind turbine power output with steady wind speed (Mathew, 2006) and (Ali, 2013)

2.6 Life Cycle Cost Analysis (LCC)

LCC is all the cost generated during the life cycle of an item (turbine). It is commonly adopted for cost saving for an investment and it implies calculation methods of total life time costs. As explained by Gluch and Baumann (2004), it is a technique which enables comparative cost assessment to be made over a specified period of time, taking into account all relevant economic factors both on terms of initial capital and future operational costs. As further analytically explained by (Nilsson & Bertling, 2007);

$$LCC = C_{inv} + C_{cm} + C_{pm} + C_{pl} + C_{rem} \quad (2.25)$$

where, C_{inv} is the cost of investment, C_{cm} is the cost for corrective maintenance, C_{pm} is the cost for preventive maintenance, C_{pl} is the cost for production loss, and C_{rem} is the cost for remainder value. Nilsson and Bertling (2007) further evaluated C_{pl} as:

$$C_{pl} = N \times P \times C_f \times C_{el} \times D \quad (2.26)$$

where N is the number of turbines, P is the electric power generated, C_f is the capacity factor ($C_f = \frac{P\ out}{Pmax}$), C_{el} is the cost of electricity and D is the downtime.

Financing wind–based projects are demanding. Considering the power generation system, investments can be high, especially for a range of 2 kW to 20 kW. The cost of a 2 kW wind turbine costs at least USD 2000 (approximately Kshs. 200,000/=) according to study conducted in Kenya by Berges (2007) in partnership with the Kenyan wind pump manufacturer- Bobs Harries Engineering Ltd. Including battery storage and installation cost, final project investment would be higher depending on the availability of local skill and expertise.

The capital cost and the cost of the energy produced by small wind turbines are still higher than large scale wind turbines according to a report given by (AWEA, 2011; IEA Wind, 2010). The cost varied widely depending on the competitiveness of the market and factors affecting installation. The global market report given by Herbert *et al.* (2012) also estimated the costs for various sub-systems of a wind turbine by using the ECON90 computer code as illustrated in Figure 2.13. Herbert *et al.* (2012) further explains that the rotor part takes the highest share accounting for more than half the cost of the turbine however, this cost can be reduced to half depending on the volume of production. Figure 2.14, 2.15 and 2.16 show the cost of separate major components (Rotor, generator and support structure respectively) of a wind turbine as found by Herbert *et al.* (2012) using ECON90 computer code.

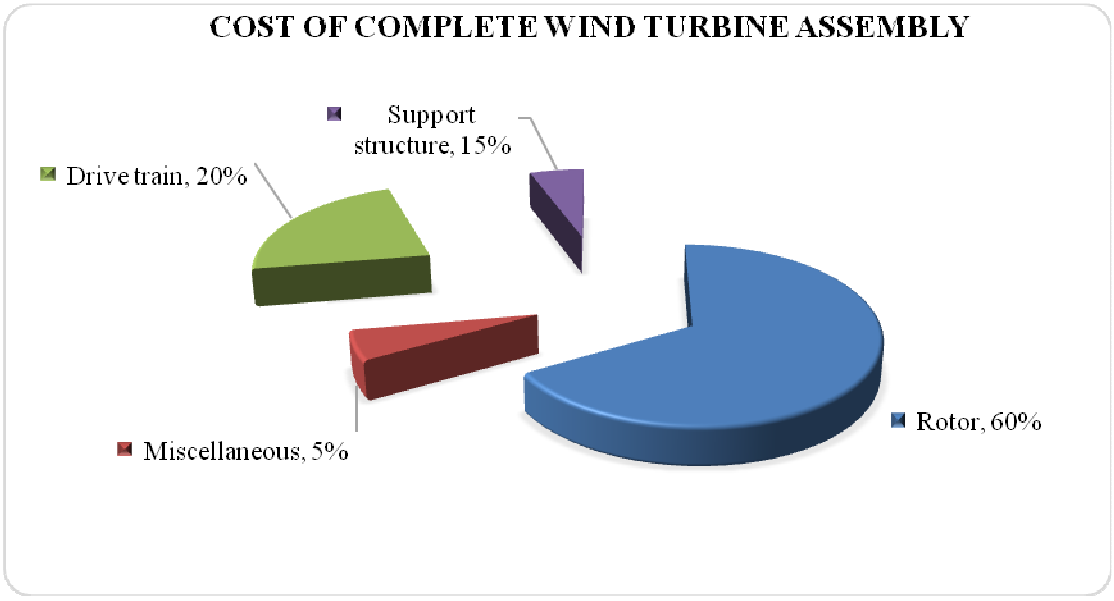

Figure 2.13: Cost of complete wind turbine components. (Herbert *et al.*, 2012).

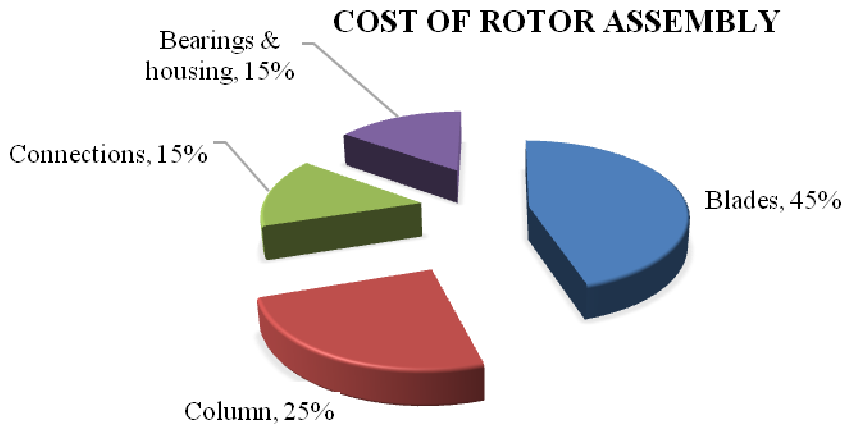

Figure 2.14: Cost of rotor assembly. (Herbert *et al.,* 2012).

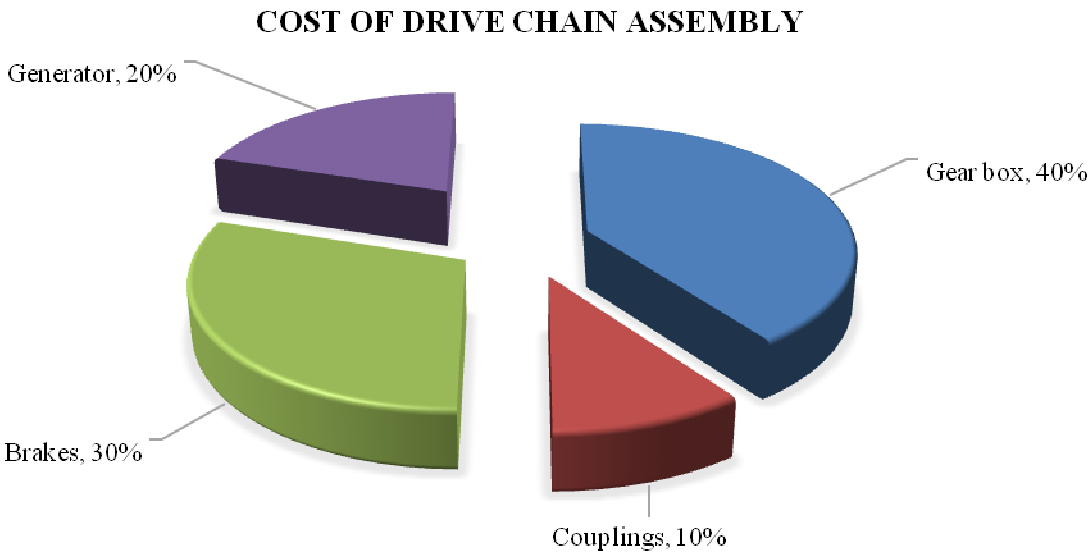

Figure 2.15: Cost of drive chain assembly. (Herbert *et al.,* 2012).

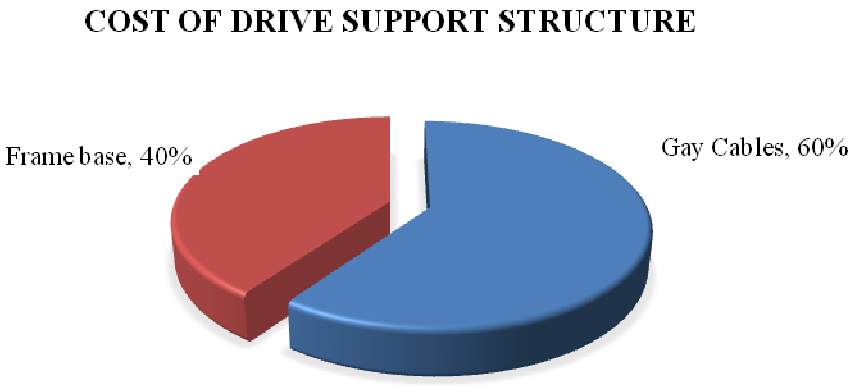

Figure 2.16: Cost of drive support structure. (Herbert *et al.,* 2012).

CHAPTER THREE

METHODOLOGY

3.1 Field and Market Research

The research started by field visits which were conducted in different local manufacturers' workshops, dealers, end users and institutions. The end result of the field visit was to come up with the SWOT analysis and to practically understand the design process. The research maximized on the weaknesses and the threats experienced by the players in the market. The stakeholders (population) identified for this study were: Nine manufacturers and dealers, six end-users, and four institutions. A full list of all the identified stakeholders of small wind energy systems are in appendix 2, 3 and 4.

Despite many stakeholders identified, only six manufacturers and dealers, five end-users and four institutions were actively involved for this research since three manufacturers were fabricating same types of wind turbines using the same technology and material where as a contact for one end user was not in service. A questionnaire was used (Appendix 1) and the mode of communication included face to face interviews, e-mails and also phone calls to those who could not be reached by either of the two.

3.2 Design Theoretical Calculations

Based on the theoretical calculations formulae, the dimensions of the rotor blades were calculated. Table 3.1 shows the theoretical designed calculated parameters and constants that were used.

Table 3.1: Theoretical design calculated parameters.

Parameter	Units	Prototype 1	Prototype 2
Output power	W	50	250
Swept area	m^2	0.7	3.2
Cut-in-wind speed	m/s	2.5	2.5
Rated wind speed	m/s	7.5	7.5
Cut-out- wind speed	m/s	15	15
Diameter	m	0.6	1.3
Height	m	1.2	2.6

CONSTANTS

Parameter	Value	Reference	Discussion
Average wind speed	5 m /s	Saoke *et al*. (2011)	----------
Solidity	≥ 0.4	Zingman (2007),	To achieve self starting
Number of blades	2	Saha *et al*. (2008), Zhao (2009) & Ali (2013)	----------
Aspect ratio	2	Johnson (1998) Modi & Fernando (1989)	H/D) = 2 (Ratio of the rotor's height to the rotor diameter
Overlap ratio	positive 25%	Modi & Fernando (1989)	Ratio of the diameter of the rotor blade to the distance which the blades overlap
Separation gap	0.03 m	Modi & Fernando (1989)	The distance of the rotor blades from the vertical axis
Cross sectional profile	Semi circular.	Albani & Ibrahim (2013)	----------
Efficiency (Coefficient of power Cp)	0.3	Paraschivoiu (2002), Manwel *et al*. (2010) and Jain (2011)	obtained from aerofoil empirical curves

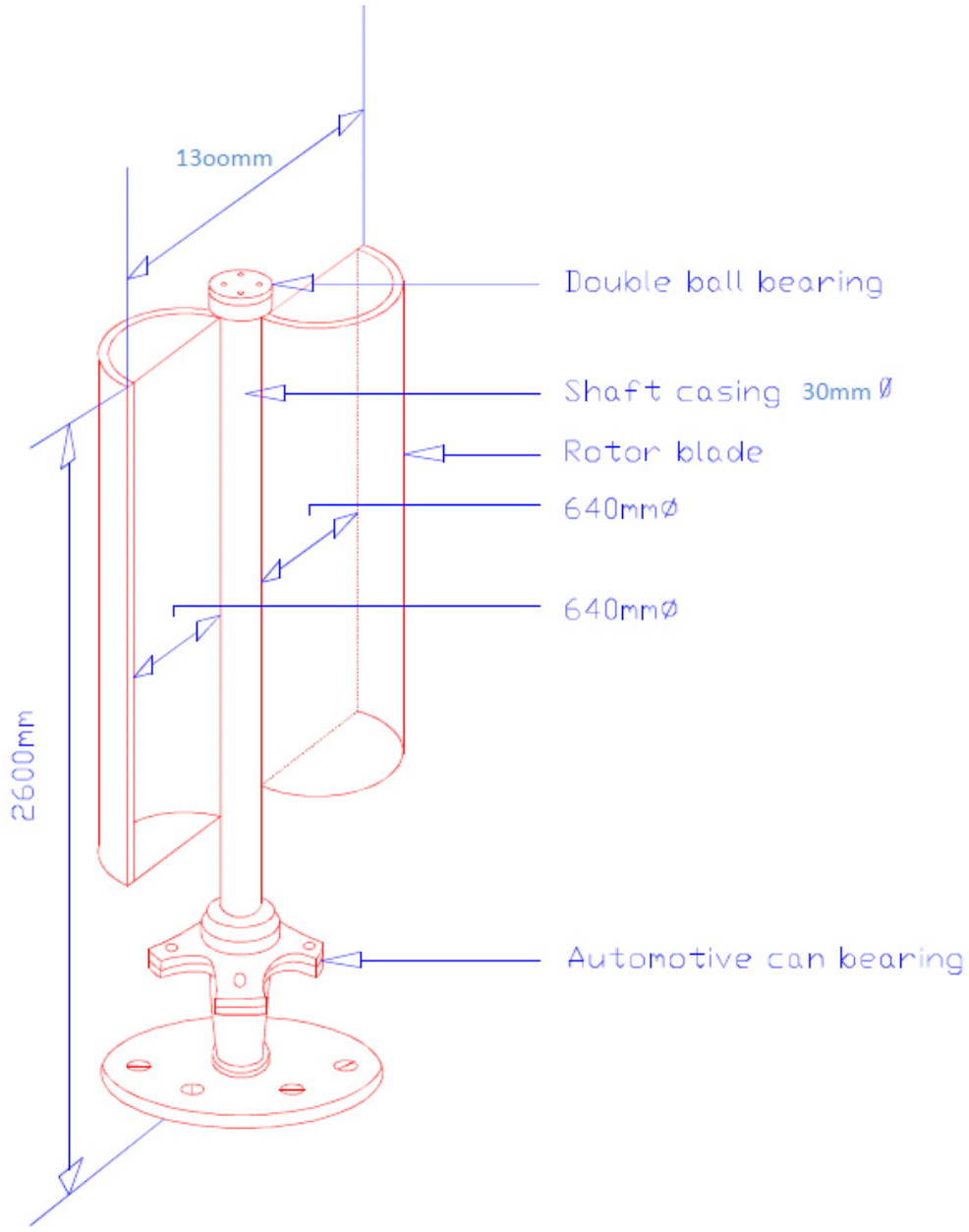

Figure 3.1: Diagram of the designed 250 W rotor blade.

3.3 Research Instruments, Material Selection and Purchase

3.3.1 Research Instruments

Table 3.2 indicates the major instruments that were used for the research and their model.

Table 3.2: Research instruments and their specifications

NAME	PICTURE	MODEL	APPLICATION
Optical Tachometer		Cdt-2000hd	Rotational speed measurements
Hand Held Anemometer		Hd 300 – extech instruments)	Wind speed measurements
Industrial Fan		Made by marshal fowler (k) limited	Wind generator

Digital Oscilloscope	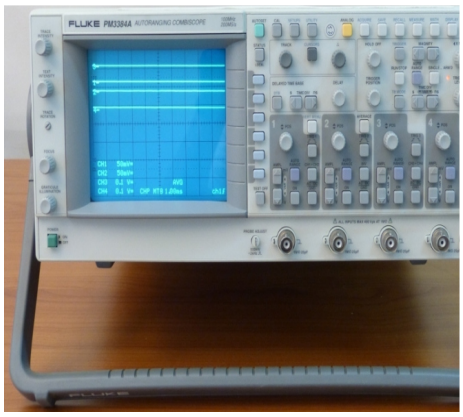	Fluke pm3384a Combiscope	Digital signal display
Digital Power Analyser		Ca8333 Chauvin arnoux	Analyse the output power in form of voltage, current and frequency.

3.3.2 Material Selection and Purchase

After analysis from the local manufacturers, the following materials were selected and purchased with respect to the materials' properties, environmental conditions as well as cost.

3.3.2.1 Rotor Blades

Fibre Reinforced Glass (FRG) was preferred simply because it is versatile, affordable, strong and durable. It does not rot or rust and hence can survive in any weather condition. It also has excellent dimensional stability which makes it hold its shape under severe mechanical and environmental stresses. Any shape can also be obtained easily from FRG mould.

3.3.2.2 Bearings

Two types of bearings were used. A Toyota Hilux car wheel bearing was used to primarily centralize the shaft. This type of bearing provided the least amount of friction, it is also generally strong and durable, has high carrying capacity as well as maintaining safe operating conditions with less maintenance/servicing. A double ball bearing 4206 A (30 mm internal diameter, 62 mm external diameter and 20 mm thickness) was also used to support the rotor rotation at the top most level. Figure 3.2 and Figure 3.3 show the two different types of bearings used.

Figure 3.2: Double ball bearing

Figure 3.3: A Toyota Hilux car wheel bearing

3.3.2.2 Rotor

The design incorporated a ‘live-shaft’. This means that the shaft rotated as part of the rotor. One of the main design aspects of the shaft were mainly for assembly and disassembly purposes. A galvanized steel (0.03 m in diameter) was used because it is cheaper than pure steel and requires minimal maintenance and at the same time is durable.

3.4 Development of the rotor blades

3.4.1 Development of the first prototype

Using the calculated design parameters obtained in Table 3.1, the first prototype was fabricated. This prototype was designed to have a power output of 50W. Some of the procedures followed included: Folding of the aluminium sheet metal of 1.5 mm thick to correct dimension of the blade, application of wax and associated chemicals to the sheet metal, separation of the glass fibre cloth from the aluminium, drilling, trimming as well as joining the blades to the shaft and the stand (tower). Plates 3.1, 3.2 and 3.3 show the blade undergoing fabrication process and a complete prototype on a stand in plate 3.4.

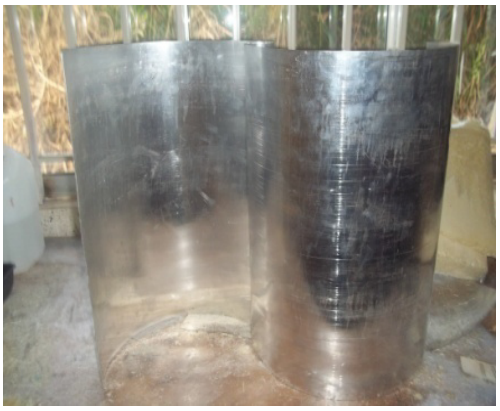

Plate 3.1: Folding of the Aluminium Sheet Metal

Plate 3.2: Application of Wax and other Associated Chemicals

Plate 3.3: Laying of the Fibre Cloth, Trimming, Smoothening and Joining of the Blades.

Plate 3.4: Complete Blade on Stand

3.4.2 Testing of the First Prototype.

The first prototype was then connected to a locally manufactured direct drive generator designed and fabricated by Akello *et al.* (2014) which had the specifications as shown in Table 3.3.

Table 3.3: Locally manufactured direct drive generator's main parameters (Akello *et al.*, 2014)

Parameter	Value	Units
Output power	1000	W
Rated speed	250	RPM
Output Voltage	24	V
No. of pole pairs	12	--
Phase number	3	--
Inner Rotor disk radius	129	mm
Outer rotor disk radius	175	mm
Rotor diameter	350	mm
Inner stator radius	129	mm
Outer stator radius	240	mm
Stator thickness	10	mm

Plate 3.5: Complete first Prototype being Tested using a Domestic Fan.

3.5 Development and testing of the second prototype

3.5.1 Development of the second prototype

After successful testing and obtaining the characteristics of the first prototype, a second prototype rotor blade was made with the parameters from Table 3.1 that would give an output of 250 W. The procedures that were involved were: A model was made from a 2 mm thick ordinary Formica curved to the designed specifications, a fibre glass mould was then made by: Cleaning the model, a releasing agent (wax) was applied on the model for easier separation of the fibre mould from the model, a gel coat was then applied which comprised of polyster resin, erosil powder and calcium carbonate ($CaCo_3$) to boost the mechanical strength. When the gel coat was dry, fibre mat was laid on the model followed with an application of polyster resin mixed with a catalyst called MEKP (Methyl, Ethyrol, and Kenton Peroxide) which is an accelerator that makes the whole solution hard and dries very fast. The strength of the mould depended on the number of layers of the fibre mat. Four layers gave the desired thickness of the blade. Plates 3.6 and plate 3.7 show the blade undergoing fabrication process. Plate 3.8 is the complete second prototype on a support.

Releasing agent and a gel coat applied on a curved Formica model

Plate 3.6: Application of releasing agent and gel on a Formica mould

Two blades already removed from the curved Formica model waiting smoothening

Plate 3.7: Blades awaiting smoothening

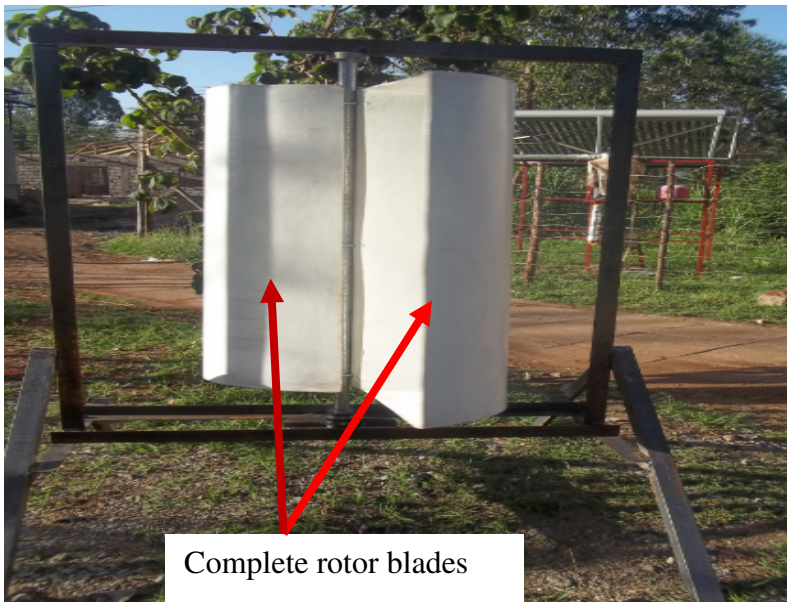

Plate 3.8: Complete second rotor prototype on a support

3.5.2 Laboratory testing of the second prototype

The rotor blade was then connected to other wind turbine's components for further testing and analysis. The other components included: The locally manufactured direct drive generator, charging control circuit (power control circuit), a lead acid battery and a 12 Vdc bulb as the load as shown in plate 3.9. The DC voltage from the power control circuit was used to charge a 12 V lead battery. The charging of the battery was monitored using a 12 Vdc bulb. The bulb came ON when the battery was 9.4 V and the light intensity increased with time as the battery got fully charged to 12 V as indicated in Plate 3.10. Figure 3.2 is the block diagram of the complete set-up.

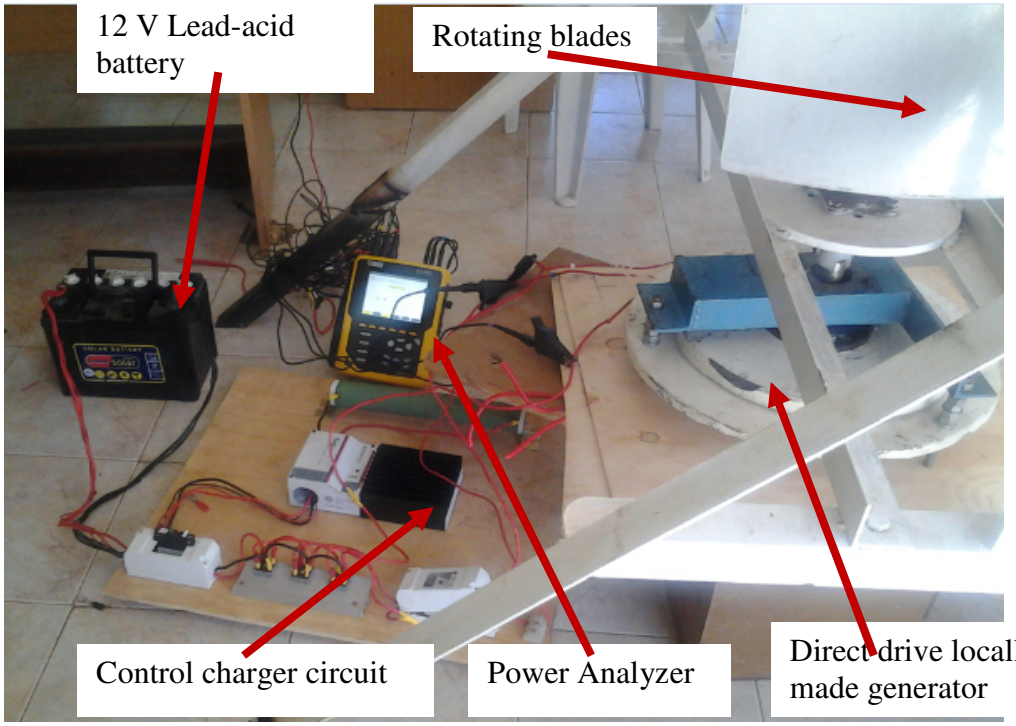

Plate 3.9: Rotor blades connected to other wind turbine components

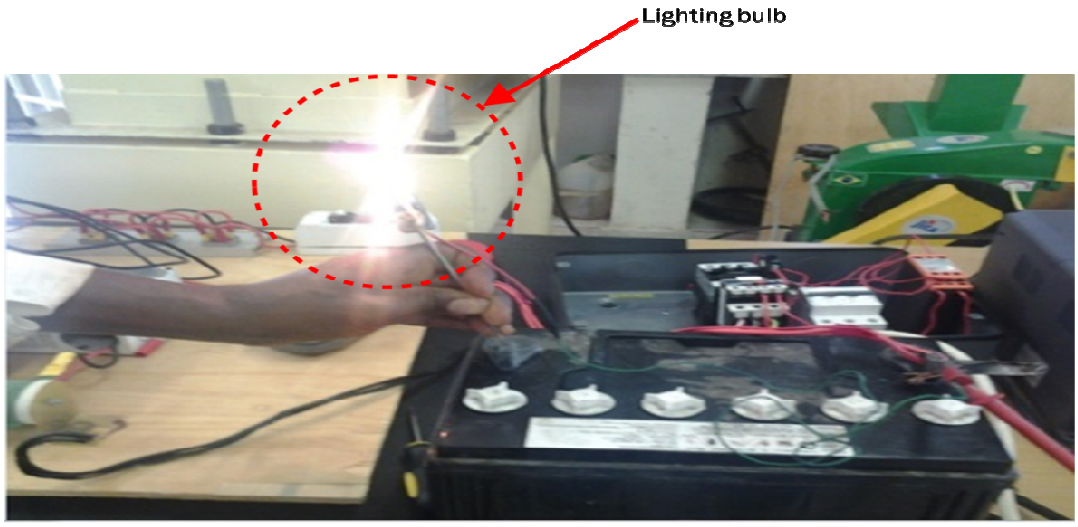

Plate 3.10: A lighting bulb from the charged 12 V lead battery.

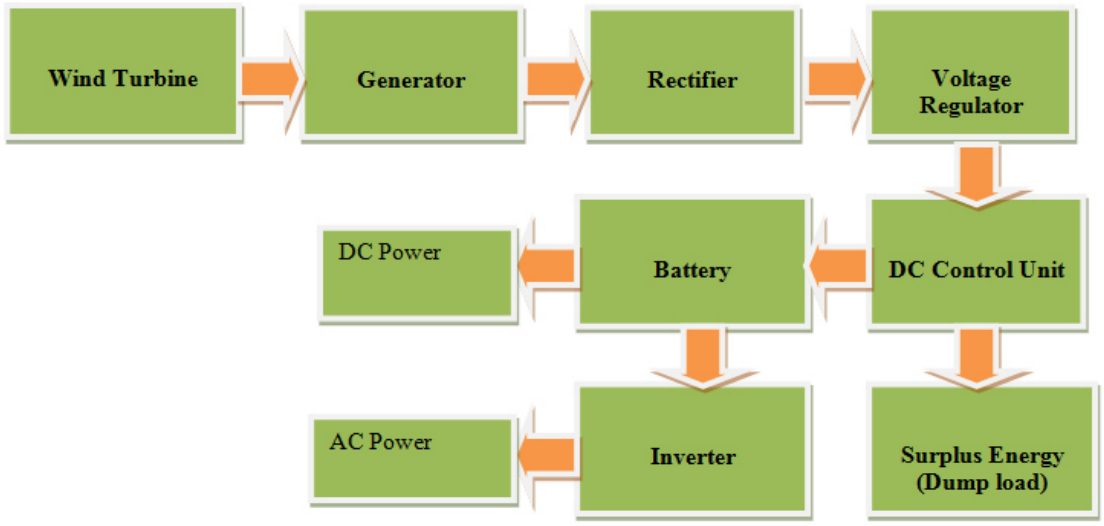

Figure 3.2: Block Diagram of the Complete Set-up

3.5.3 Field testing of the second prototype

The rotor blade was then tested at the field. This was to get the performance characteristics of the turbine when exposed to the environmental conditions. Ngong hills was the selected site where other commercially grid connected turbines are installed. The power station is located in the northern foothill, near Ngong town in Kajiado county, approximately 35 km southwest of Nairobi city –Kenya. The peak of the Ngong hills is at 2460 m (8070 feet) above the sea level. (Courtesy of Aeronautical chart for Nairobi area)

Plate 3.11: Rotor blade connected to a direct drive generator at Ngong' wind farm

Figure 3.3 summarises the process (step-by-step) of activities that were involved in the research for the development of the Savonius rotor blades.

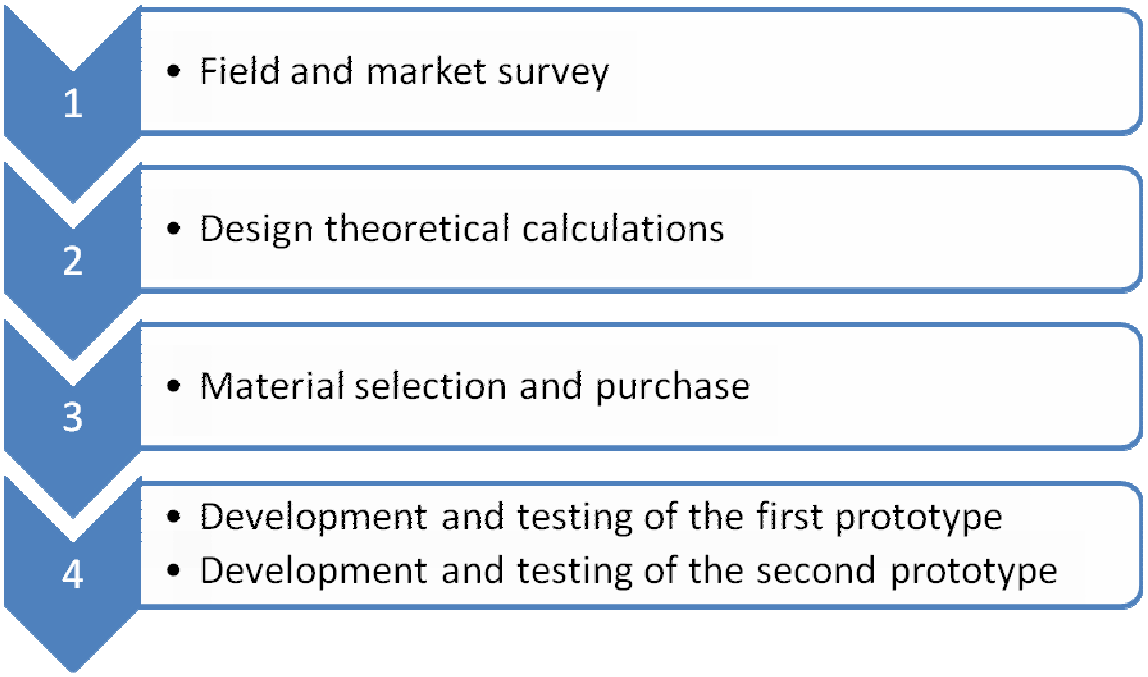

Figure 3.3: Flow of Activities for Savonius Blade Development and Testing.

CHAPTER FOUR

RESULTS AND DISCUSSIONS

4.1 Result from the Field Survey

4.1.1 Major Players (Manufacturers and Dealers)

For a long period of time Kijito Wind Power Ltd had been dominating in the manufacturing of wind mills locally as others import, supply and install as a small product line according to a research on Capacity Development for Promoting Rural Electrification Using Renewable Energy- Training Needs Assessment Survey on Small Wind Energy Systems, conducted by Magambo and Mwenda (2013). However, the major local manufacturers and dealers had increased to twelve in number by the time of the research. List of all the manufacturers and dealers identified in Kenya are in Appendix 2. However, six local manufacturers and dealers who were involved in this study are shown in Table 4.1.

Table 4.1: Local manufacturers of small wind energy systems used for the research

	Name of the player	Main product	Location
1	Riwik East Africa	Wind turbines	Thika
2	Craftskills Wind Energy International LTD	Wind turbines/ and wind mills	Nairobi
3	Kijito Wind power LTD	Wind mills	Thika
4	Windgen &Powergen Renewable Energy LTD	Wind turbines	Nairobi
5	Kigima High-tech Metal Works	Wind mills	Kiserian
6	Powertechnics (K) LTD	Wind turbines, wind mills and BOS components	Nairobi

Powertechnics (K) LTD is the only company that imports all the parts of a wind turbine. The company assembles and installs for their customers as demanded. RIWIK East Africa manufactures 90% of the wind turbine and all its balance of systems including a generator and an inverter in their workshop. This manufacturer however, complained of heavy taxation still on importation of the permanent magnet for fabricating a direct drive generator despite the government's incentives to allow duty free importation of renewable energy hardware as mentioned in Sessional paper No.4 (2004). This is the only manufacturer who locally fabricates the direct drive generator. Kijito Wind Power LTD, Craft skills wind Energy International LTD modifies the used geared motors to match the rating of their wind turbines. Windgen Renewable Energy LTD and Kigima High-Tech Metal Works LTD use gearing system and/or import the complete generator. Kijito Wind power LTD and Kigima High-tech Metal Works locally manufacture purely windmills, Riwik East Africa and Windgen and Powergen Renewable Energy LTD locally manufacture purely wind turbines while Craftskills Wind Energy International LTD and Powertechnics (K) LTD deal with both wind mills and wind turbines depending on the customer's demand.

The maximum hub height obtained was 19 m, however, this depended on the site of installation and the available wind speed. The standard average hub height stands at 10-15 m high. The average output voltage (Vdc) stands at 12 V to 48 V for a wind turbine, and above that range is for a wind mill since it requires more torque. Appendix 5 show photographs of some of the products found in the market. Table 4.2 shows the manufacturers' products and specifications found from the field survey.

Table 4.2: Wind Turbines' Types, Manufacturers and Technical Specifications.

Brand names	Manufacturer	Country of origin	Rated power	Units	Output voltage (Vac)	Cut-in-speed (m/s)	Cut-out-speed (m/s)	Hub height (m)
Kijito	Kijito	Kenya	10-70	m^3 /day	--------	2.5	45	9-12
Airflow	Riwik East Africa Ltd	Kenya	350-1000	W	24/48	3	12.5	10
Craftskills	Craftskills Int.	Kenya	300-3000	W	12/24/48/98/360	2-4	10-15	12
Maglev Wind turbines	Powertechnics	China	Any	W	24	2-3	13	Depends on site of installation
Twiga, Simba	Windgen	Kenya	200-1000	W	12/24	3.2-3.5	12.5	9-19
Ndovu Rhino	Windgen	Kenya	200-1000	W	12/24	3.2-3.5	12.5	9-19
Kigima	Kigima High-tech metal works	Kenya	10	W	----	----	----	10

4.1.2 End-users (Customers)

The end-users identified were either individuals or institution based who use the wind turbines/wind mills for lighting or pumping water. The end-users who were directly involved in the information for this research were six in number even though twelve were identified as given in Appendix 4. Three customers use the wind system as a wind turbine and the remaining three use the wind energy system as a wind mill. All the customers interviewed were satisfied with the system's availability and reliability including a customer whose system was not functioning at the time of interview. All the customers said they would not hesitate to recommend the energy system to other people. Their major challenge however is the poor after sales services and also unreliable wind source hence forcing two institution based customers to boost their supply with diesel generators in cases of high demands. Of all the customers, only one had a maintenance contract with the supplier and was supplied with an operational manual. The rest do seek for assistance when the system starts malfunctioning or breaks down.

The major problems encountered by the customers were: Broken and worn out rotor blade, corrosion of the blades, loose bolts and nuts, collapse of the rotor hubs especially during wind storms, worn out bearings, burnt dump loads, controller and battery failure, armature failure and malfunction of the control card as well as rotor imbalance. All the customers were trained on the operation and maintenance of the system upon installation and given a warranty of two years within which the customer buys the spares for replacement if needed though servicing cost remains free during the period.

4.2 Laboratory Results from the first Prototype

Table 4.3 shows the results that were obtained after connecting the rotor blades to the direct drive locally manufactured generator. All the parameters were measured except Power, Cp and TSR that were calculated from the measured parameters using equations.

Table 4.3: Laboratory Results from the first Prototype

Wind speed	Blade rotational speed		Voltage	Current	Power (W)		Cp	TSR
m/s	RPM	Torque (N)	V	I (A)	P_B	Pw	C_P	TSR
0	0	0	---	---	0	0	0	0
2.1	0	0	---	---	0	0	0	0
2.69	4.5	14.9	---	---	1.1	2.5	0.13	0.02
3.25	5.4	21.7	---	---	2.0	4.4	0.13	0.02
4.92	10.8	49.8	4.1	1.3	9.0	15.3	0.18	0.02
5.44	10.9	60.9	3.8	1.6	11.1	20.7	0.16	0.02
5.88	11.3	71.1	5.3	1.6	13.4	26.1	0.15	0.02
6.07	11.4	75.8	5.3	1.6	14.4	28.7	0.15	0.02
6.31	11.5	81.9	5.4	1.7	15.7	32.3	0.15	0.02
7.62	11.7	119.4	7.2	1.9	23.3	56.9	0.12	0.02
7.82	11.9	125.7	7.3	2.0	24.9	61.5	0.12	0.02
8.07	12.3	133.9	7.4	2.2	27.4	67.5	0.12	0.01
8.57	12.3	151.0	7.9	2.3	31.0	80.9	0.11	0.01
9.48	12.7	184.8	9.2	2.5	39.1	109.5	0.11	0.01
10.32	12.9	219.0	9.9	2.7	47.1	141.3	0.10	0.01
10.61	13.2	231.5	10.0	3.0	47.52	153.5	0.09	0.01
11.3	12.3	262.6	11.3	3.1	42.8	185.4	0.07	0.01
11.84	11.8	288.3	11.6	3.5	39.9	213.3	0.06	0.01
12.9	11.5	342.2	14.9	3.6	22.8	275.9	0.02	0.01
13.7	11.1	386.0	15.9	4.1	19.1	330.5	0.02	0.01

The cut-in-wind speed for the first prototype was found to be at 2.7m/s which gave a torque of 14.9 N. However useful electrical power of 9.0 W was obtained at 4.92m/s with an average line voltage of 4.1 V, and an average line current of 1.3 A. The maximum Cp obtained was 0.18 at a TSR of 0.02. However the Cp obtained at the rated wind speed reduced to 0.12 with a constant TSR ratio of 0.2. The power curve for the results in Table 4.3 is presented graphically in Figure 4.1.

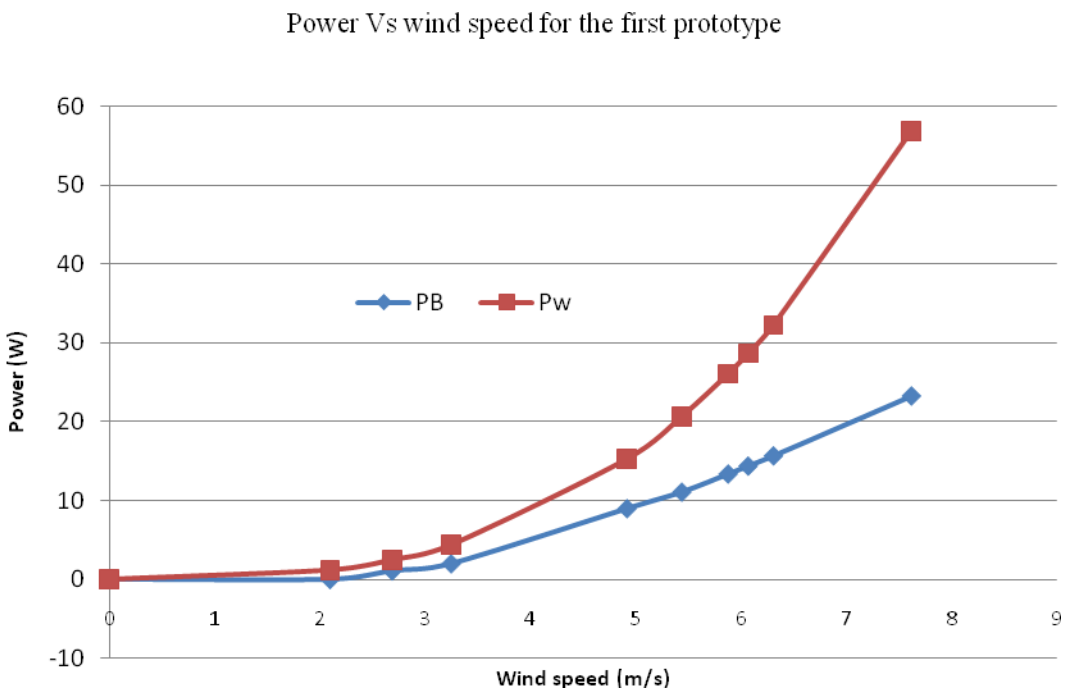

Figure 4.1: Laboratory power curve for the first prototype.

From initial calculation of wind power equation (equation 2.7) and using the rated wind speed of 7.5 m/s, the power output measured was 19.5 W instead of the theoretical 44.6 W. The calculated performance obtained from the results was;

$$E = \frac{P_B}{P_W} \times C_P \times 100\% \qquad (4.1)$$

$$= \frac{19.5}{44.6} \times 0.3 \times 100\%$$

$$= 0.13 \text{ or } 13\%$$

4.3 Laboratory Results from the Second Prototype

Table 4.4: Laboratory Results from the Second Prototype.

Wind speed	Blade rotational speed		Voltage	Current	Power (W)		Cp	TSR
m/s	RPM	Torque (N)	V	I (A)	P_B	Pw	Cp	TSR
2.1	20.98	11.2	3.4	0.7	3.9	5.4	0.22	0.5
2.69	42.31	18.4	6.7	1.1	13	11.4	0.34	0.5
3.25	59.3	26.9	12.7	1.2	26.6	20.2	0.40	0.8
4.92	74.9	61.6	29.4	1.5	76.9	70	0.33	1.0
5.44	80.4	75.3	32.6	1.8	101	94.6	0.32	0.8
5.88	87.5	88.0	41.7	1.9	128.4	119.4	0.32	0.8
6.07	90.3	93.8	42.9	1.9	141.2	131.4	0.32	0.8
6.31	94.3	101.4	45.3	2.1	159.3	147.6	0.32	0.8
7.62	98.3	147.8	62.1	2.2	242.2	259.9	0.28	0.8
7.82	100.2	155.7	66.7	2.3	260.0	281	0.28	0.7
8.07	103.9	165.8	68.8	2.5	287.1	308.8	0.28	0.7
8.57	110.8	187	80.3	2.5	345.3	369.8	0.28	0.7
9.48	117.9	228.8	102.8	2.6	449.6	500.6	0.27	0.7
10.32	122.8	271.1	122.6	2.7	554.9	645.7	0.26	0.7
10.61	125.7	286.6	128.4	2.8	600.4	701.7	0.26	0.6
11.3	130.4	325.1	145.6	2.9	706.5	847.7	0.25	0.6
11.84	137.2	356.9	154.5	3.1	816.1	975.2	0.25	0.6
12.9	142.7	423.7	171.3	3.5	1007	1261	0.24	0.6
13.7	150.2	477.8	202.4	3.5	1196	1510	0.24	0.6

The cut-in-wind speed was below the rated wind speed of 2.5 m/s. At 2.1 m/s an electrical power of 3.9 W was obtained with an average line voltage of 3.4 V, line current of 0.7 A and a torque of 11.2 N. The designed rated power output was 250 W at 7.5 m/s and at this wind speed, power output of 242.2 W was obtained at 62.1 V and 2.2 A. The highest C_p obtained was 0.40 at a TSR of 0.8. At the rated wind speed the C_p obtained was 0.28 at a TSR of 0.8. Figure 4.2 is the graphical representation of Table 4.4.

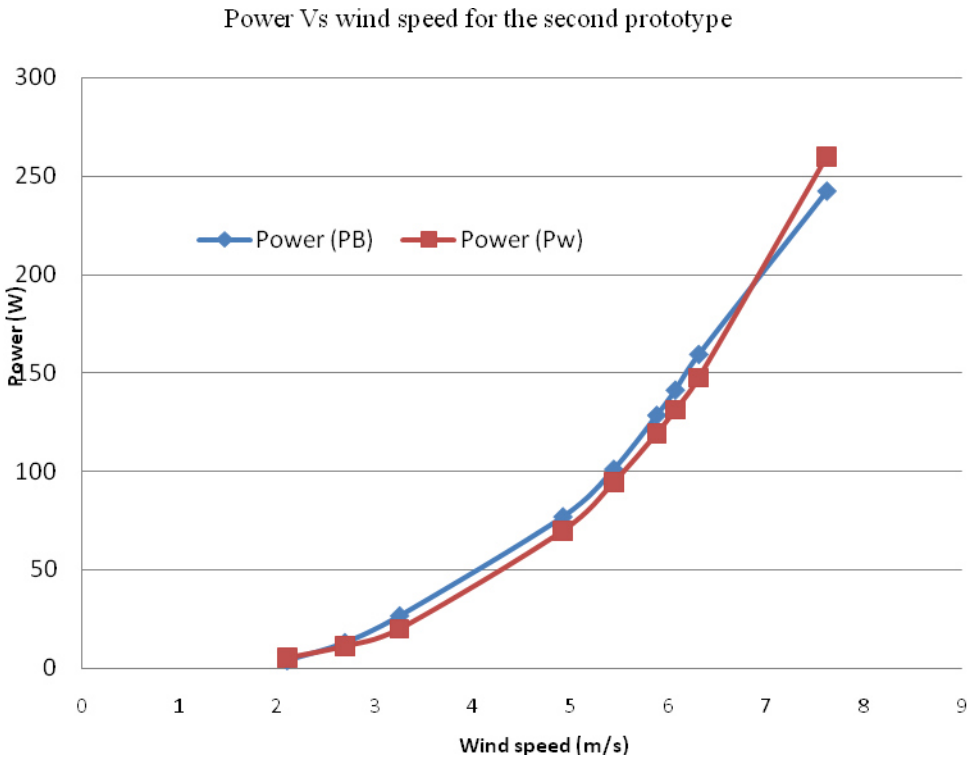

Figure 4.2: Laboratory power curve for the second prototype.

Figure 4.2 shows that the actual power (power of the turbine) from the measurements (P_B) was slightly lower than the theoretical power (power of the wind, P_w). The cut-in-wind speed was below the rated wind speed of 2.5 m/s since at 2.1 m/s an electrical power of 3.9 W and a torque of 11.2 N were obtained. The maximum power output obtained was 242.2 W at 7.5 m/s instead of a theoretical power of 259.9 W. The calculated performance from the result was 40% when equation 4.1 was used. This came as a result of improvement on the development. The first prototype had five layers of fibre mat as compared to the second prototype which had four layers hence hindered the rotational speed of the first prototype though it had a better starting torque suitable for water pumping. The second prototype was fabricated in a fibre glass workshop with assistance of the fibre glass technicians hence improved on the quality of the fabrication.

4.4 Field Testing of the Second Prototype

Field testing was done at Ngong hills on November 24th, 2014 from 10:23 A.M to 5:40 P.M where the horizontal axis wind turbines are currently installed. On the day of testing, the weather was very calm and the highest wind speed recorded was 6.44 m/s. The wind speed measured on that day is in Appendix . Table 4.5 shows the torque and voltage measurements that were obtained on the day of field testing.

Table 4.5: Field test result of the second prototype

Wind speed	**Blade rotational speed**		**Voltage**	**Current**	**Power (W)**		**TSR**	C_P
m/s	**RPM**	**Torque (N)**	**V**	**I (A)**	**Pm**	**Pw**	**TSR**	C_P
1.46	7.56	5.4	---	---	0.7	1.8	0.1	0.11
1.53	7.56	6.0	0.93	0.003	0.8	2.1	0.1	0.10
2.08	12.95	11.0	2.72	0.54	2.4	5.3	0.1	0.13
2.78	33.69	19.7	4.93	1.32	11.0	12.6	0.3	0.26
3.05	48.28	23.7	5.15	2.17	19.1	16.7	0.3	0.34
3.7	73.63	34.9	8.57	2.86	42.8	29.8	0.4	0.43
3.58	74.88	32.6	8.46	2.85	40.7	27.0	0.5	0.45
4.58	80.82	53.4	13.9	3.87	71.9	56.4	0.4	0.38
5.73	90.84	83.6	15.52	4.77	126.6	110.5	0.3	0.34
6.26	108.96	99.8	26.30	4.05	181.1	144.1	0.4	0.38
6.44	129.70	105.6	36.73	3.69	228.2	156.9	0.4	0.44

The blade started rotating at 1.53 m/s, electrical power of 0.8 W and mechanical power of 6.0 N was measured. However the useful power was obtained at 2.08 m/s with a power output of 2.4 W. The rated wind speed was not attained on the day of testing but

the power output at the highest measured wind speed of 6.44 m/s was 228.2 W. The highest C_P obtained was at 0.44 at a TSR of 0.4. This result was slightly higher than the laboratory results from the second prototype. Figure 4.3 is a graphical representation of the power curve from the field test results.

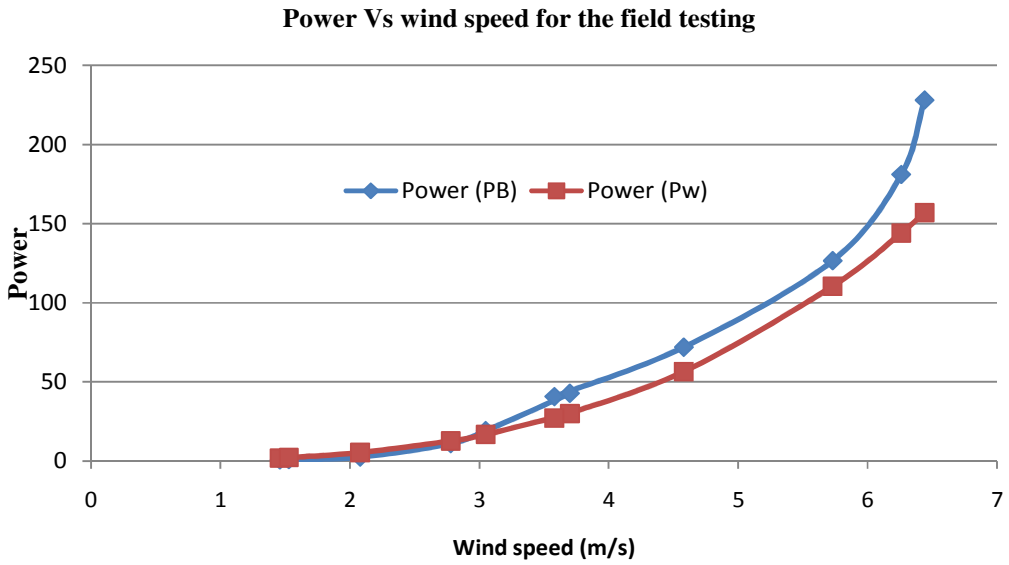

Figure 4.3: Field test power curve of the second prototype.

Calculation from equation 4.1, it was found that testing which was done at Ngong Wind farm resulted to a performance of 44%. This was because the place is at a higher height of 2460 m (8070 ft) above sea level with less turbulence. All the sections of the blade were also exposed to the wind as compared to the laboratory testing where the surface area of the blade could not fit in front of the wind source. In the laboratory, the wind source was channelled to only one direction which is advantageous to HAWTs. However for VAWTs like Savonius, different change in wind direction as experienced in the field test had a positive impact on the blades hence higher stable power was achieved.The 44% in performance is also higher than the conventional C_P of 30% which was achieved in 2011 by Jain hence an objective of a more efficient blade was achieved.

4.5 Analysis of the Power Curves

From Table 4.5, a cut-in wind speed was found to be at 1.46 m/s which was below the designed cut-in wind speed of 2.5 m/s. This was achieved because of the material used. RFG is known to be very light and requires very little wind speed for it to start. Amongst the rotor blades found in the market, only one manufacturer uses glass fibre to produce the horizontal axis blades. However they did not have the testing results of their wind turbines. A local assembler's (importer) field test result was found to have 36% efficiency as indicated in the Figure 4.5.

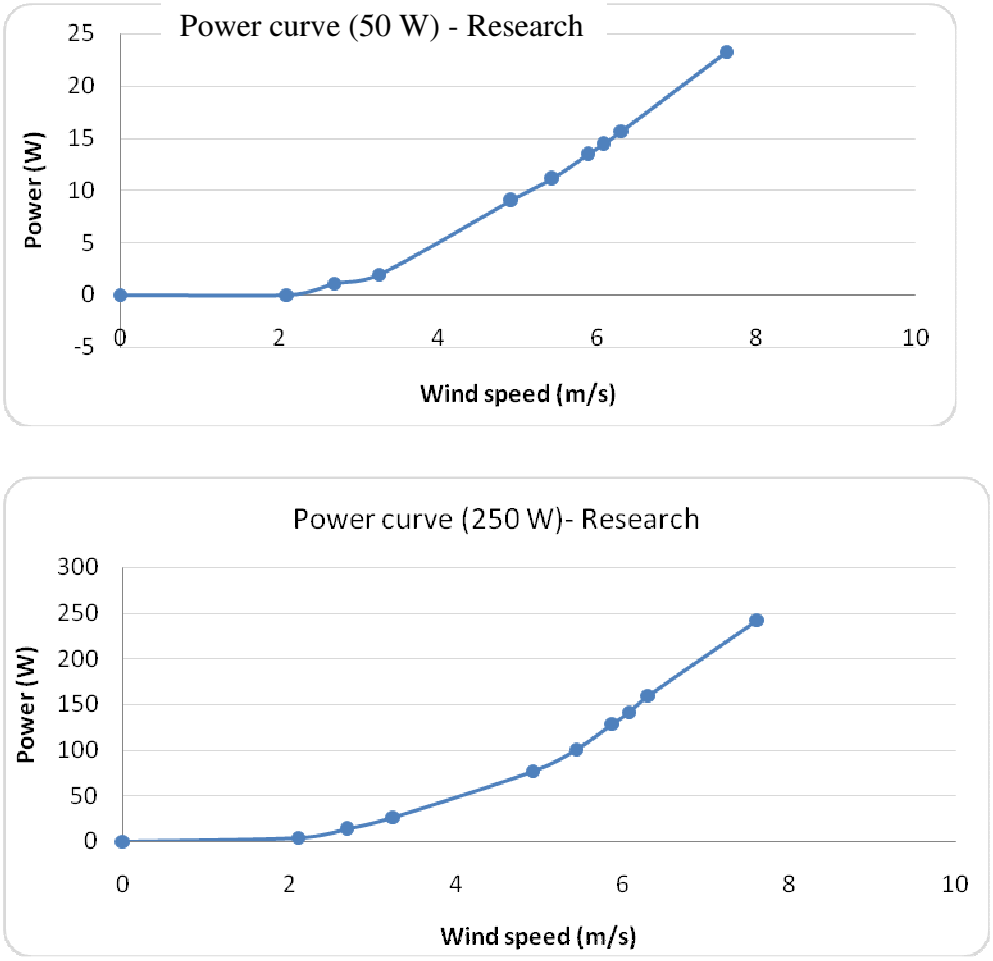

Figure 4.4: 50W and 250W power curves from the research

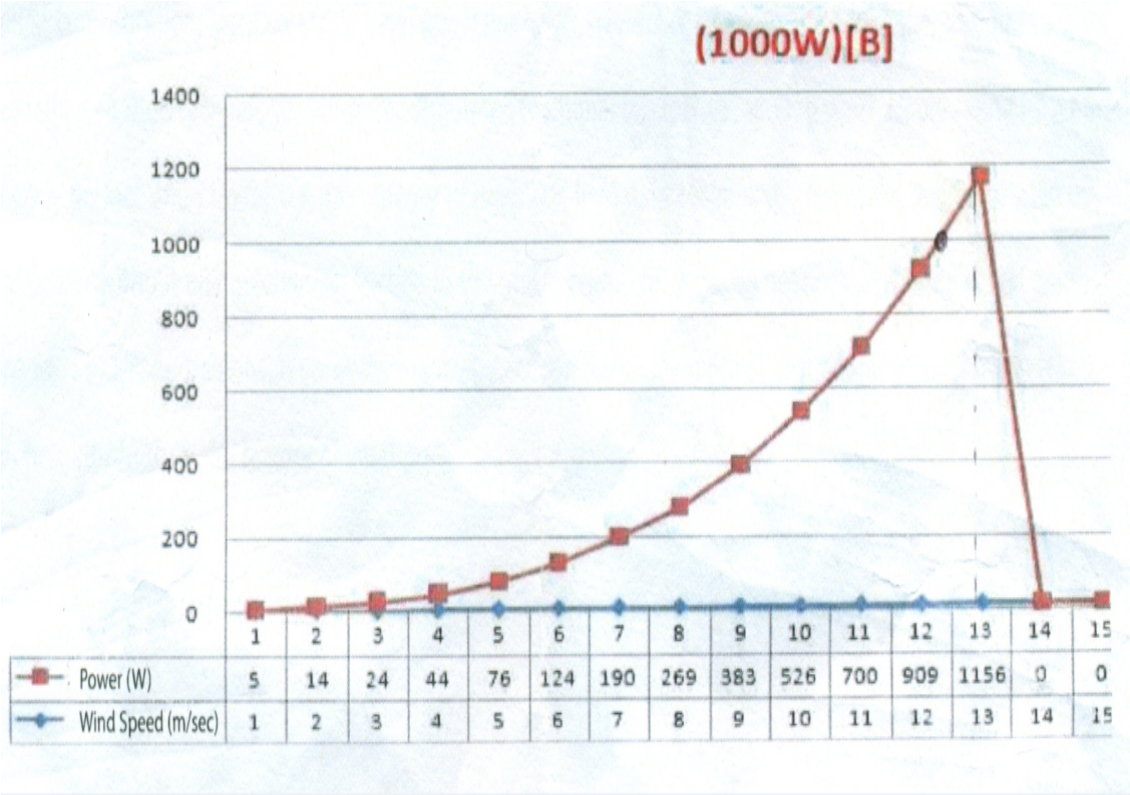

Figure 4.5: Power Curve from a Local Assembler. (Powertechnics (K) LTD brochure)

The power performance of a wind turbine is usually illustrated using the $C_p \sim \lambda$ curve as shown in Figure 4.6. The highest C_p was obtained during the field test though high roughness was experienced by the turbine as shown on the field test curve. At stable wind speeds the highest C_p obtained was 0.45 at a TSR of 0.4.

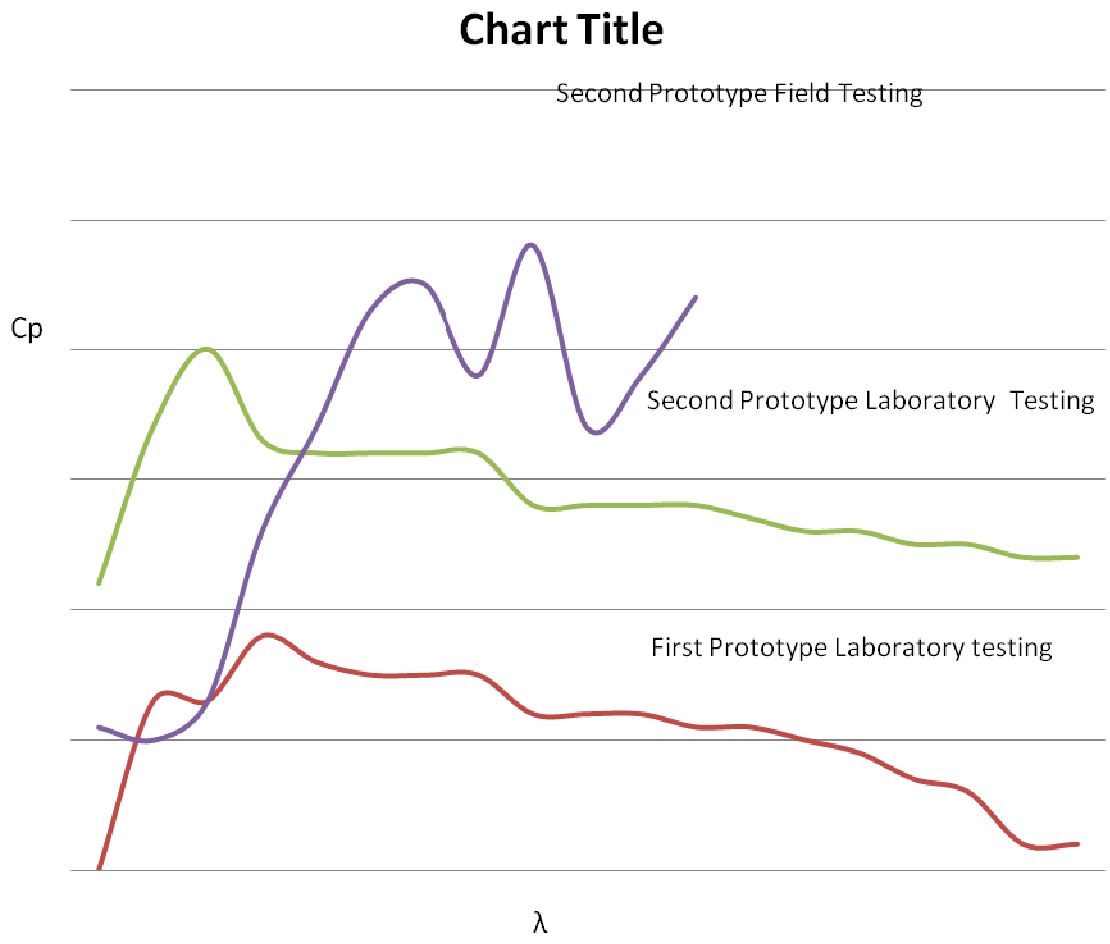

Figure 4.6: $C_P \sim \lambda$ curve

4.6 Economic Analysis.

The cost of fabrication of the rotor blades was then compared with a quotation obtained from a local assembler (RIWIK EA LTD).

Table 4.6: Cost of Producing the Rotor Blades in a Local Kenya's Market.

Installed wind turbine capacity (W)	Rotor	Generator	Miscellaneous	Support structure	Application (load)	Application-facility	Total cost (Kshs)
200-300	192,500	70,000	35,000	52,500	Lighting and small domestic appliances	Domestic households	350,000
400	247,500	90,000	45,000	67,500	Lighting and domestic appliances	Domestic households.	450,000
700-900	302,500	110,000	55,000	82,500	Lighting, entertainment and ICT equipment	Schools and hospitals	550,000
1000-1500	412,500	150,000	75,000	112,500	Lighting, entertainment and ICT equipment	Schools and hospitals	750,000
2000-3000	660,000	240,000	120,000	180,000	Lighting, entertainment and ICT equipment	Schools and hospitals	1.2 M

Table 4.7: Cost Incurred for the Fabrication of the Rotor Blades for the Research

Component/Description	**Amount (Kshs)**
Fibre reinforced Glass chemicals and associated materials	45,000
Labour for blades fabrication	12,000
Support structure and base material	10,000
Labour for support structure and base fabrication	3,000
Bearings and housing	7,000
Fitting materials (Bolts and nuts)	1,000
Transportation	5,000
Total	**83,000**

Table 4.6 and 4.7 are graphically represented as shown in Figure 4.7 and Figure 4.8.

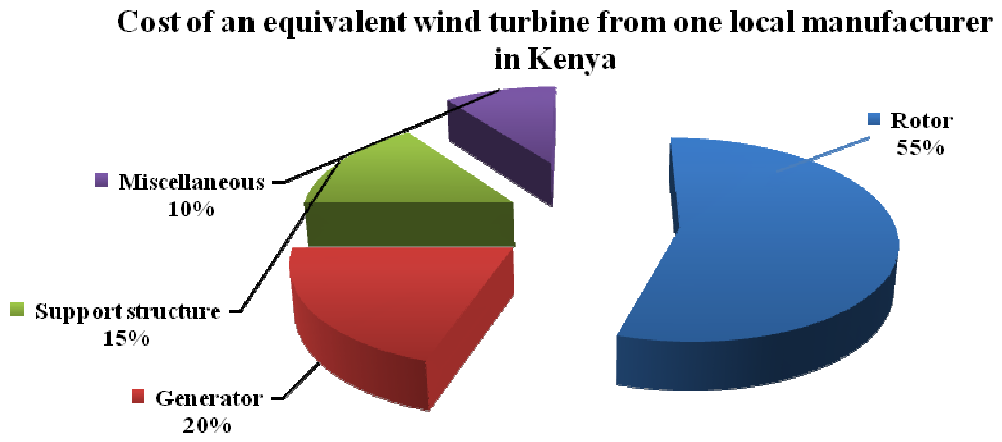

Figure 4.7: 200-300 W Local Wind Turbine Production Costs.

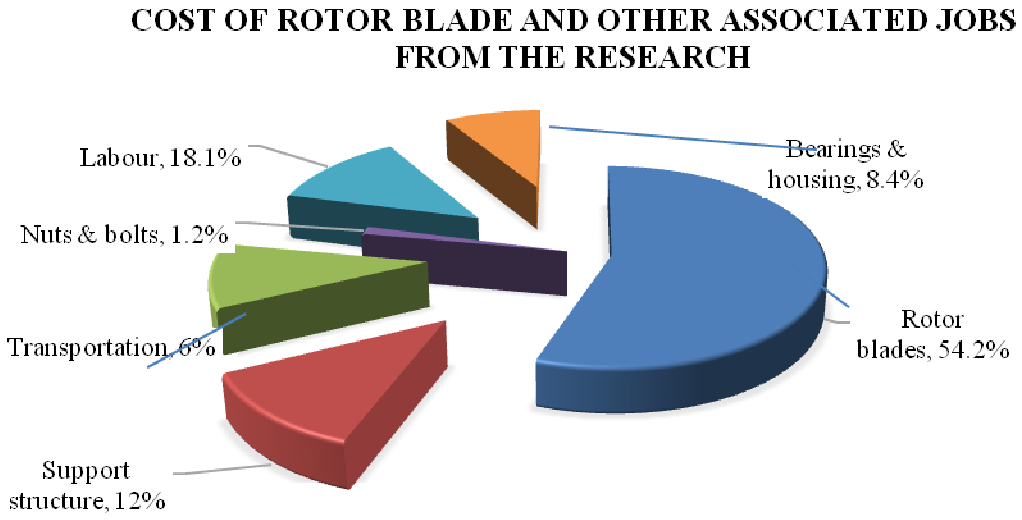

Figure 4.8: Cost of Rotor Blade and other associated Jobs from the Research.

From the research, the total amount used to produce the complete rotor blade and its accessories were as shown in Table 4.7 and presented graphically in figure 4.8 which shows similarity with the one generated by Herbert *et al.* (2012) .i.e. the rotors' cost was more than half of the total cost.

From the field survey, only one local manufacturer (RIWIK EA LTD) was free to disclose the quotation and the profit percentage margin of a complete wind turbine. From this supplier, a rotor blade of the same rating costs Kshs. 192,500/= and Kshs. 350,000/= for a complete wind turbine including 27% profit. The researcher's blade cost was Kshs. 83,000 which resulted to a 56.8% cheaper than the ones in the market. This is due to the fact that the materials used were all locally available.

CHAPTER FIVE

CONCLUSIONS AND RECOMMENDATIONS

5.1 Conclusions

The government supports the development of small wind energy market and there are small wind energy programmes being undertaken by the government to promote the adoption. However, very little is known on VAWTs. Only one dealer (Powertechnics (K) LTD) assembles VAWTs whereas the rest manufacture and / assemble HAWTs. The policies were also found not fully implemented when a local manufacturer (RIWIK E.A) complained of higher taxation imposed on importation of the permanent magnets for fabrication of the direct drive generators instead of free tax importation as mentioned in Sessional paper N0.4 (2014).Most of the knowledge and skills available in the industry have been acquired through on- job- trainings, personal initiatives and practical trials especially in local manufacturing.

The market penetration of small wind turbines was found to be very small. This is because the turbines are made or assembled on order by the manufacturers who then install them. The ministry of Energy is implementing the energy act No. 12 of 2006 partially by enforcing the solar water heating systems and the solar PV regulations. However, the small scale wind turbines sector is ignored.

The Savonius rotor blade that was designed was found to be practical after producing electricity that could charge a 12V dc lead battery for domestic application. The cut-in wind speed for the second prototype was found to be less than 2.5 m/s, i.e. at 2.1m/s, an output power of 3.9 W during laboratory testing and 2.4 W during field testing was obtained improved the performance from 28% to 44% when the turbine was tested in the field.

The cost of developing the designed blade was reduced by 56.8% compared to Kenya's price of a similar rating. This was achieved by fabricating the blades using the local available materials. It was therefore possible to locally develop a small wind conversion technology that is affordable, efficient and adaptable for Kenya's average low wind speed.

5.2 Recommendations

Sensitization of wind energy systems should be done through academic institutions, workshops and even through government initiatives like sponsoring more projects. Sensitization on fibre technology should also be done for further embracement in many applications. This recommendation may take time, however short courses should be facilitated for dealers, manufacturers and other interested service providers.

Introduction of the gearing system in the transmission system would further increase the production output. However research for such a system is recommended which would consider factors like noise, installation cost and maintenance cost for user affordability and needs. Fabricating the live shaft using steel facilitated the assembling and disassembling of the rotor blades with ease. However, raising the shaft (tower) would improve the wind catchment of the rotor, and hence the general performance of the machine.

Safety of such a wind turbine is necessary for higher wind speeds, therefore, further research on more advanced cost effective control strategy with the installation of an electronic controller which would adjust the rotation speed to present wind speed.

Savonius rotor with central shaft between the end plates was found to improve the coefficient of power and assist in obtaining uniform coefficient of static torque. I therefore recommend a future study on the performance of the turbine with respect to the central shaft.

REFERENCES

Abraham, J. P., Plourde, B.D., Mowry, G. S., Mincowcyz, W. J., &Sparrow, E. M. (2012). *Summary of Savonius wind turbine development and future applications for small scale power generation.* Minessota: American Institute of physics.

Akello, P.A., Ochieng, F.X., & Kamau, J.N. (2014). Performance analysis of a direct drive permanent magnet generator for small wind energy applications. *Journal of sustainable research in engineering, 1*(3), 1-9.

Albani, A, & Ibrahim, M.Z. (2013). Preliminary development of prototype of Savonius wind turbine for application in low wind speed in Kuala Terengganu. *International journal of scientific &technological research, 2*(3), 102-108.

Ali, M. H. (2013). Experimental Comparison study for savonius wind turbine of two & three blades at low wind speeds. *International journal of modern engineering research*, 2978-2986.

Ali A., Golde S., Alam F. & Moria H.,(2012). Experimental and computational study of a micro vertical axis wind turbine. *Procedia Eng, 49*, 254–62.

Altan, B. A. (2008). The use of a curtain design to increase the performance level of Savonius wind turbine. *Journal of renewable energy*, *35*(4), 821-829.

Altan, B. D., Atilgan, M., & Ozdamar, A. (2008)..An experimental study on improvement of Savonius rotor performance with curtaining. *International journal of experimental thermal and fluid science, 32*(8), 1673-1678.

Altan, B. D., & Atilgan, M. (2012). A study on increasing the performance of Savonius wind rotors. *Journal of Mechanical Science and Technology, 26*(5), 1493-1499. Retrieved from: www.springerlink.com/content/1738-494x

Ayieko, Z., (2011). Rural Electrification programme in Kenya: Lighting up rural Kenya. AEI practitioner's workshop- Dakar, Senegal.

Berges, B., (2007). *Development of small wind turbines*. Lyngby, Denmark: Technical University of Denmark.

Burton, T., Jenkins, N., Sharpe, D., & Bossanyi, E. (2011). *Wind energy handbook*. (2nd ed.). Chichester, UK: John Wiley and sons.

Castelli, R.M., Englano, A. & Benini, E. (2011). The Darrieus Wind Turbine: Proposal for a new Performance Prediction Model based on CFD. *Elsevier energy*, *36* (8), 4919-4935.

Colly, G., Mishra, R., Rao, H. V., & Woolhead, R. (2010). *Effects of rotor blade position on vertical Axis Wind Turbine Performance.* International Conference on Renewable Energies and Power Quality. Paper 5 ICREPQ'10. Granada: Spain.

Cooper, P. (2010). Development and analysis of Vertical Axis Wind Turbines: Wind power generation and wind turbine design: WIT press. 277-328.

Emmanuel, B, Jun, W. (2011). Numerical Study of a Six-bladed Savonius Wind Turbine. *Journal of Energy Engineering, 133*(4), 044503.

Gluch, P. & Baumann, H., (2004). The life cycle costing (LCC) approach: a conceptual discussion of its usefulness for environmental decision-marketing, *Elsevier.*

Gogoi, R., Ballabh, R. &Das, K. (2013). Experimental investigation of three- stage Savonius Rotor with concentrator. *International journal of Mechanical Engineering and Research*, *3*(4), 401-406.

Government of Kenya, (2004). Sessional Paper No. 4 on Energy: Final report. Ministry of Energy. Nyayo House, Nairobi. Retrieved from www.energy.go.ke

Government of Kenya, (2015). Draft National Energy and Petroleum Policy. Ministry of Energy and petroleum. Retrieved from www.energy.go.ke.

Government of Kenya, (2015).The Energy Bill. Ministry of Energy. Retrieved from www.energy.go.ke.

Government of Kenya, (2006). The Energy Act. Ministry of Energy and petroleum. Retrieved from www.erc.go.ke

Grinspan, A. S., Suresh, K. P., Saha, U. K. & Mahantra, P. (2003). *Performance of Savonius wind turbine rotor with twisted bamboo blades.* Proceedings of 19th Canadian Congress of Applied Mechanics, 2, pp.412-413: Calgary, Alberta, Canada.

Gupta, R., Biswas, A., &Sharma, K.K. (2008). A comparative study of a three bucket Savonius rotor with a combined three bucket Savonius- three bladed Darrieus rotor . *International Journal of Renewable Energy*, *33*(9), 1974-1981.

Hau, E. (2006). *Wind turbine, fundamental, technologies Application and Economics*. (2nd ed.). Berlin Heidelberg: Springer.

Herbert, J., Dale, E., &Thomas, D. (2012). *A retrospective of VAWT technology*. New Mexico: Sandia National library.

Harries, M. (2002). *An introduction to Kijito wind pumps in Afrepren*. Occasional paper number 10: Afrepren, Nairobi, Kenya.

Harries, M. (2002). Disseminating wind pumps in rural Kenya-meeting rural water needs using locally manufactured wind pumps. Energy policy article in wind pumps.

Hayashi, T. (2005). Wind tunnel test on a different 3-D Savonius rotor. *Japan Society of mechanical Engineers International Journal, 48*, 9-16.

Jain, P. (2011). *Wind Energy Engineering*. New York: The McGraw-Hill Companies.

Johnson, C. (1998). Practical wind generated electricity. Retrieved from: http://mb-soft.com/public/wind .html.

Kamoji, M. A., Kedare, S.B., & Prabhu, S. V. (2007). *Experimental investigation on modified Savonius rotor.* AIAA Applied Aerodynamics conference, (pp. 768-780).

Kamoji, M. A., Kedare, S. B. &Prabhu, S.V. (2009). Experimental investigations on single stage modified Savonius rotor. *Applied Energy*, *86*(7), 1064-1073.

Kolachana, S. (2012). *A computational framework for the design and analysis of Savonius wind turbine:* Madras- Chennai: Indian institute of technology.

Letcher, T. (2010). *Small scale wind turbines optimized for low wind speeds*. 24thHayes graduate research forum. Ohio: The Ohio state University.

Magambo, K. &Mwenda, J. (2013). *Capacity Development for Promoting Rural Electrification Using Renewable Energy-Training Needs Assessment Survey on Small Wind Energy Systems.* Nairobi: Rencon Associates LTD.

Manwel, J. F., McGowan, J. C. & Rogers, A. L. (2009). *Wind Energy Explained*: Theory, Design and Application (2nded.). Great Britain: John Wiley and Sons LTD.

Mathew, S. (2006). *Wind Energy Fundamentals, Resource Analysis and Economics.* Vela New York: Springer.

Menet, J. (2004). A double step Savonius Rotor for local production of electricity: A design study. *Journal of renewable energy, 29*(11), 1843-1846.

Miau, J.J., Liang, S.Y.,Yu, R.M, Hu, C.C., Leu, T.S., Cheng, J.C., &Cheng, S.J, (2012). Design and test of a vertical-axis wind turbine with pitch control. *Applied Mech Mater, 225,* 338-343.

Modi, V..J., & Fernando, M.S.U.K. (1989). Performance of the Savonius Wind Turbine. *Journal of solar energy engineering*, *111*(1), 71-78.

Mohamed, M.H., Janiga, G., Pap, E., & Thévenin, D., (2010). Optimization of Savonius turbines using an obstacle shielding the returning blade. *Journal of Renewable Energy, 35*(11), 2618-2626.

Nelkon, M. & Parker, P. (1995). *Advanced level physics.* (7th ed.). London: Longman international Education.

Nilsson, J., & Bertling, L., (2003). Maintenance management of wind power systems using condition Monitoring systems- Life cycle cost analysis for two case studies*, IEEE Transactions on Energy Conversion, 22*(1), 223-229.

Paraschivoiu, I. (2002).*Wind turbine design: With emphasis on Darrieus concept.* Montreal: Polytechnic international press.

Peter, J. S., & Richard, J. C. (2012). Wind turbine blade design. *Energies,* 5, 3425-3449.

Kumar, R. & Prashant, B. (n.d.). Solidity study and its effects on the performance of a small scale HAWT. *Impending power demand and innovative energy paths* , 290-297.

Riwik. (2011). Production and Installation Manual. Website of the company, Riwik East Africa LTD. Retrieved from:www.riwikeastafrica.com

Saha, U. K., & Rajkumar, M. J. (2006). On the performance analysis of Savonius Rotor with twisted blades. *Journal of Renewable Energy, 31*(11), 1776-1788.

Saha, U. K., Thotla, S.,& Maity, D. (2008). Optimum design configuration of Savonius rotor through wind tunnel experiments. *Journal of Wind Engineering and Industrial Aerodynamics*, *96*(8), 1359-1375.

Saoke, C.O., Kamau, J.N., & Kinyua, R. (2011). Wind speed distribution, estimation of wind shear exponent and roughness parameter for Juja, Kenya. *Journal of Environmental Sciences and Resource Management.* (2), 121-137.

Sargolzaei, J., & Kianifar, A. (2007). Estimation of the power ratio and torque in wind turbine Savonius rotors using artificial neural networks. *International journal of Renewable Energy, 1*(2), 14-16.

Savonius, S.J. (1931). The S-Rotor and its applications. *Journal of mechanical engineering, 53*(5),333-338.

Sharma, P. K. (2001). *Vertical axis wind turbine: Design, Fabrication and Experimental Study of Savonius Rotor and Straight Blade Wind Turbines*. B. Tech. Project Report, Mechanical Engineering Department, IIT-Guwahati.

Sheldai, R.E., Feltz, L.V., & Blackwell, B.F., (1978).Wind tunnel performance data for two-and three-bucket Savonius rotors. *Journal of Energy, 2*(3), 160-164.

Simonds, M., & Bodek, A. (1964). *Performance test of a Savonius rotor*. Micro-fiche reference library, Technical Report T10, Quebec: McGill University.

Solanki, C. S. (2009). *A practical guide for beginners in renewable energy technology.* New Delhi: PHI learning Private LTD.

Twidell, J., & Weir, T. (2006). *Renewable Energy Resources*, (2nded.). New York: Taylor and Francis.

Wekesa, D. W., Wang, C., Wei, Y., Zhu, W. (2016). Experimental and numerical analysis of small scale turbine aerodynamic performance at a plateau terrain in Kenya. *Journal of renewable Energy, 90,* 377-385.

Widodo, W.S., Chin, A.C., Haeryip, S., & Yuhazri, M.Y. (2012). *Design and Analysis of a 5 kW Savonius Rotor Blade.* Get view. Supergen'09, Nanging pp 1-8. Retrieved from:www.getview.org.

www.practicalaction.org

Zingman, A. (2007). *Optimization of a Savonius Rotor Vertical Axis Wind Turbine for use in Water Pumping Systems in Rural Hinduras.* Arong O. Zingman. New Delhi: PHI learning Private LTD.

Zhao, Z.Z., Zheng, T, Xu, X.Y., Liu, W.M., & Hu, G.X. (2009). *Research on the improvement of the performance of Savonius rotor based on numerical study sustainable power generation and supply.* The proceedings insupergen'09.Nanging.

APPENDICES

Appendix 1: Sample questionnaire

SECTION 1: DEVELOPER INFORMATION

Name of organization/Institution:	
Organization type:	
Physical Address:	Telephone Numbers:
E-mail Address:	
Name of CEO/Principal/Director:	
Name of interviewee:	Designation of the interviewee:
E-mail of the interviewee:	Telephone numbers of the interviewee:
Name of interviewer	Date of interview:
Main activity: ……..…..	
Major products/Services: …….	
Number of employees: ……..	
Number of years involved in the wind business: ……	
Type of wind energy system: ……	

PART A: MANUFACTURERS

1. What is the overall business activity?

What type of wind energy system (s) do you manufacture/import/supply?

Where do you get your wind energy systems from? (Manufacture, Import, local supplier)

Where in Kenya is the technology installed, how many and for what application?

Model number	County/nearest town	Quantity	Application	Year of installation	Installation cost	Current status

2. Description of the rotor blade used:
3. Description of the transmission system used
4. Performance rating of the wind turbine:
5.

Model number	Rotor system	Transmission system	Tower	Power production	End user view of performance	Further development

(Use a rating of 1=Excellent 2=Good 3= Average 4=Poor)

6. Provide general information of the wind energy system

Model Number	Rated capacity	Rotor diameter	Cost of installation	Cost of rotor blade	Cost of tower	Cost of wind turbine	HAWT/VAWT

7. Please provide details of technical staffs under your employment

Name	Position (Engineer, Technician, artisan)	Academic qualifications	Academic institutions

8. Provide the SWOT analysis (STRENGTH, WEAKNESS, OPPORTUNITY and THREATS) that are encountered in your daily manufacturing/importing/distribution of the energy systems

Component	Advantages or opportunity	Challenges/disadvantages	Mainly affects which model
Rotor system			
Transmission system			
Tower			

Power production

9. What are the Policies, legal and regulatory framework governing your firm

Component	Policy	Legal and regulatory	Financing	Sales and distribution	Operation & maintenance	Others (Specify)

10. Do you provide training on operation and maintenance to users and provide the operation and maintenance manual?

11. Do you offer preventive maintenance service contracts? Please provide the details below.

Typical technical problems:_____
Number of customers under maintenance contracts:_____
Average cost per visit:_____
Technical trainings for the technical staffs (i.e. in house, in country, abroad or others). Specify the content.

PART B: CUSTOMERS (END-USERS)

1. Who is the sponsor/operator/owner of the facility?_____
2. Please provide the details of the supplier of your wind energy system:_____
3. When was your wind energy system installed and commissioned?:_____
4. What is the maximum electricity demand of the main loads?

Load	Rating (W, kW)	Average no. of hours of operation/day	Demand (kWh/day)

5. Provide details of the installed wind power systems as below:

Rated capacity of wind power	Number of wind turbines	Total battery capacity	Rated capacity of the charge controller	Rated capacity of the inverter	Power supply (a.c/d.c.)

6. What were the major reasons to invest in the wind energy system described above?
7. Who introduced you to the wind energy system installed?
8. What was the total installation price for your system?
9. Did you receive training on operation and maintenance of the wind system and the respective manuals?
10. How is the operation and maintenance of the system carried out?

	Yes/NO	Please provide details
Maintenance contracts/ after sales service provided? By Manufacturer/Distributer		
Maintained by user/?		
How often is maintenance done by user/ manufacturer/ Distributer		
Any other option used		

11. Do you maintain any data/ records in relation to the wind energy system installed? (performance/ monitoring data, maintenance records e.g. parts replaced, system faults e.g. controller, battery, blades e.t.c.)_____
12. How satisfied are you with the performance of the systemduring its period of operation?

1=very dissatisfied 2=fairly dissatisfied 3=50/50 4= fairly satisfied 5=very satisfied

	1	2	3	4	5
Reliability (Does the system meet your energy needs always?)					
Availability (frequency of the breakdowns)					
Availability of wind resource to generate power					
Cost of operation and maintenance					
Comment on the overall performance of the system					

13. Would you recommend any one else to invest in a wind energy system?_____

PART C: GOVERNMENT INSTITUTIONS:

1. What is your mandate in the development and utilization of small energy wind systems in the country?_____
   _____
2. Are there policies/ regulatory support mechanisms that have been put in place to support dissemination of wind energy systems in the country?
   _____
   _____
3. Are there any incentives that are currently in use in Kenya?_____
   _____
4. Are there any investments incentives that currently apply in Kenya?
   _____
   _____
5. Are there government policies or regulations for the management of wind energy systems in Kenya?_____
   _____

Appendix 2: List of Local Manufacturers.

	Name	Main products	location
1	Kijito Wind power Ltd	Wind mills	Thika
2	Craftskills Wind Energy International Ltd	Wind turbines	Nairobi
3	Davsan Engineering Works	Wind mills	Eldoret
4	Powergen Renewable Energy Ltd	Wind turbines	Nairobi
5	Riwik East Africa Ltd	Wind turbines	Thika
6	Kigima high-tech Metal works	Wind mills	Kiserian
9	Access Kenya Limited	Wind turbines	Kisumu
12	Chloride Exide (K) Ltd	Wind turbines	Nairobi

Appendix 3: List of Local Dealers

	Name	Product
1	Powertechnics (K) Ltd	Wind turbines and balance of systems (BOS) components
2	Davis & Shirtliff (K) Ltd	Wind turbines and BOS components
3	Energy Outfitters Ltd	Wind turbines and BOS components
4	Powerpoint systems (E.A.) Ltd	Wind turbines and BOS components
5	Access Energy Ltd	Wind turbines and BOS components
6	Kenital Kenya Ltd	Wind turbines and BOS components
7	Trusun Power Ltd	Wind turbines and BOS components
8	Battery World	VAWT and BOS components
9	Adept Pacesetters	BOS components
10	Centre for Alternative Technologies	BOS components
11	African Energy	BOS components
12	East African Wind Energy Limited	Wind turbines and BOS components
13	EcoSolar Options Ltd	Wind turbines and BOS components
14	Socabelec East Africa Ltd	Wind turbines and BOS components
15	Solar Teknowledge & Renewable Energy Ltd	Wind turbines and BOS components

	Name	Product
16	Sun Power Technologies Ltd	Wind turbines and BOS components
17	Adept Pacesetters	Wind Systems and BOS components
18	Energy Alternatives Africa Ltd	Wind Systems and BOS components
19	Hari Krusan Electric	Wind Systems and BOS components
20	Solar Homepower	Wind Systems and BOS components
21	Telesales Solar	Wind Systems and BOS components
22	Greenleads Limited	Wind Systems and BOS components
23	Greenmillenia Energy Ltd	Wind Systems and BOS components
24	Trusun Ltd	Wind systems and BOS components
25	Continuum Africa	Wind systems and BOS components

Appendix 4: List of End users

	Name	Type of Wind energy system
1	St. Francis Xavier Girls Secondary school	Wind turbine
2	Daughters of Charity	Wind turbine
3	Maarifa centre	Wind turbine
4	Patterson Memorial Secondary School	Wind turbine
5	Ewangan Oloishobor School	Wind turbine
6	Alastair Campbell Residence	Wind turbine
7	Idris Yusuf Farm	Wind turbine
8	Ole Nguso Garden resort	Wind turbine
9	Ol Pejeta Conservancy	Wind mill
10	Alfred Cherwon Farm	Wind mill
11	Mary Kalulu farm	Wind mill
12	Peter Njau farm	Wind mill

Appendix 5: Wind Products in the Market

5.1: Locally manufactured rotor blades of a wind turbine.

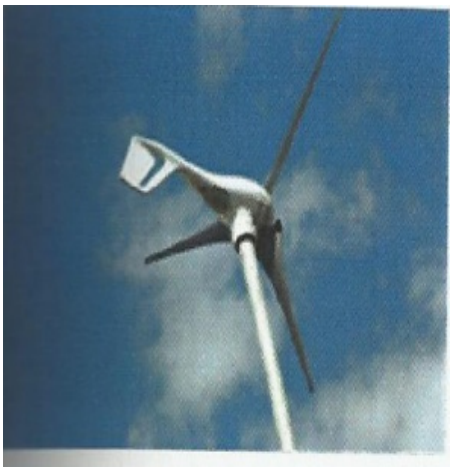

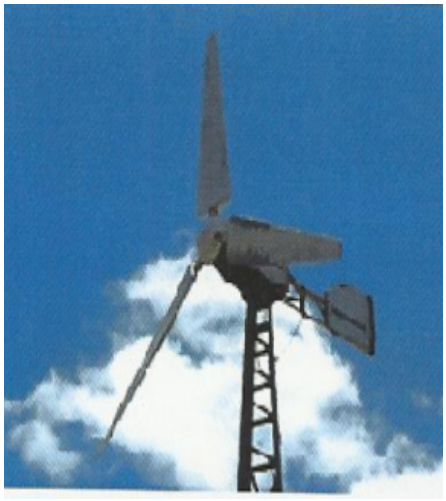

5.2: Locally manufactured rotor blades for wind mills.

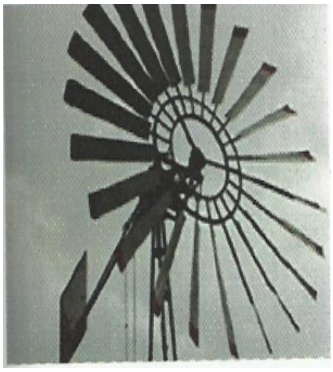

5.3: Imported Maglev rotor blade of a wind turbine.

Appendix 6: Typical Application of Wind Turbines

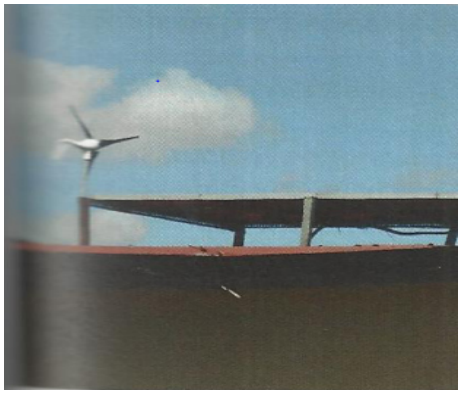

Wind turbine & Solar energy (Hybrid system-School)

Wind turbine used for lighting (home)

Wind turbine used (water pump)

Wind turbine (communication mask)

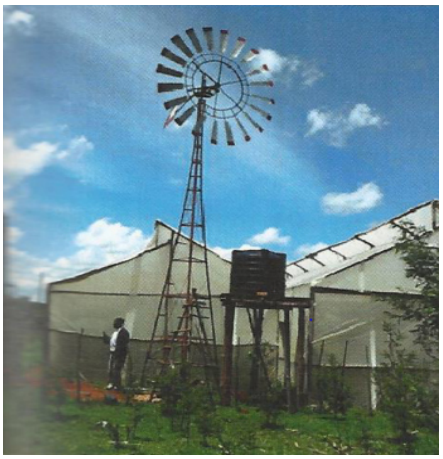

Wind mill (pump water)

Maglev wind turbine (Power an estate)

Wind turbine for lighting

Appendix 7: Locally available Balance of Systems (BOS).

(a) Batteries

(b) Inverters

(c) Dump loads

(d) Controllers

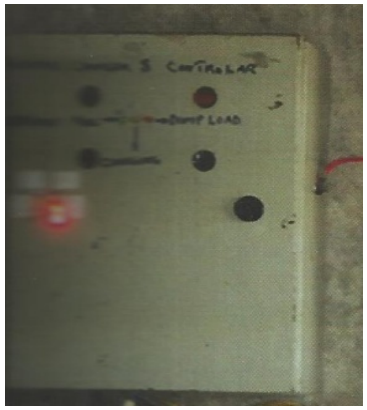

Appendix 8: Complete Controller circuit used in the research

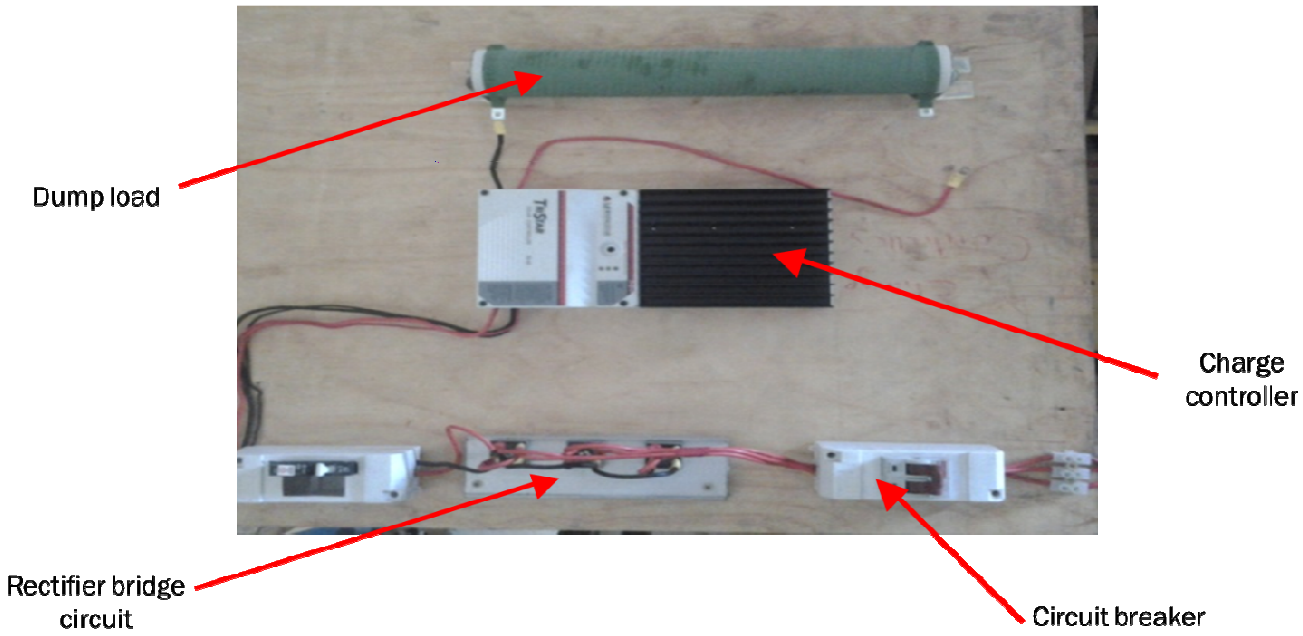

Appendix 9: Fabrication process photographs

Fabrication of the first prototype in the research laboratory (JKUAT)

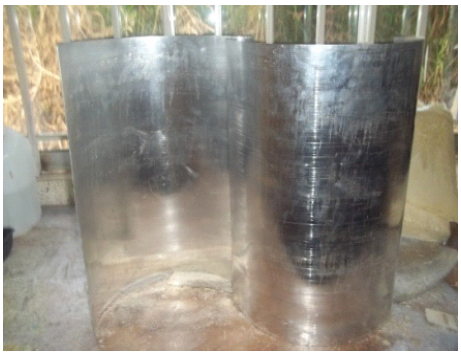

Folding of aluminium sheet metal

Application of resin and GRF layers

Fabrication of the improved blade (prototype)

Live shaft and stand fabrication

Complete rotor blades on a stand

Appendix 10: Ngong Wind Park Wind Speed Measurements

DAY OF TESTING USING SONIC ANENOMETER.

DATE: 24th Nov, 2014 INTERVAL: 10 Minutes

Table 2: Ngong wind park measurements (Courtesy of KENGEN Ngong wind farm)

Time	WTG 1 (m/s)	WTG 2 (m/s)	WTG 3 (m/s)	WTG 4 (m/s)	WTG 5 (m/s)	WTG 6 (m/s)
8:50	3.3	2.3	2.3	3.1	2.6	2.2
9:00	3.1	2.6	3.1	3.6	3	2.5
9:10	2.8	2.2	2.8	3	2.9	3
9:20	2.7	2.5	2.5	2.8	2.4	2.3
9:30	2.4	1.9	1.5	2	1.6	1.5
9:40	2	2.4	2.6	2.8	2.5	1.4
9:50	2.4	2	1.9	2	2	1.6
10:00	1.7	2.8	3.2	3.1	3	2.6
10:10	3.5	2.1	2.3	2.8	2.7	2.3
10:20	3.2	2.4	2.1	2.6	2.2	2.3
10:30	3	2.2	2.1	2.7	2.6	2.5
10:40	2.9	2.4	2.3	2.7	2.8	2.6
10:50	3.8	2.1	2.2	3	2.4	2.9
11:00	2.7	2.1	2.3	2.9	2.3	2.8
11:10	3.3	2.1	2.1	2.7	2.4	2.5
11:20	2.6	2	2.3	2.8	2	2.4
11:30	2.5	2.3	2.4	2.7	2.5	3.3
11:40	2.8	2.2	2.4	2.8	2.7	3.4
11:50	3.1	1.8	2.1	2.3	2.3	2.2
12:00	1.9	1.6	1.5	1.6	1.7	1.9
12:10	1.7	0.7	0.6	0.3	0.4	0.5
12:20	0.6	1	1.1	1	0.8	0.8
12:30	0.5	2.9	2.4	2.7	2.4	2.6
12:40	2.7	2.8	3.2	3	3.1	3.3
12:50	3.1	3.2	3.5	3.5	3.9	3.9
13:00	3.2	5	5.2	5.4	5.3	5.9

13:10	4.4	4.9	5.3	5.4	4.9	5.4
13:20	5.9	5.3	5.2	5.3	5.2	5.4
13:30	5.2	5.7	5.7	5.4	5	5.9
13:40	6.3	3.8	4	4.4	4.5	4.7
13:50	3.7	2.9	3.4	3.5	3	3.6
14:00	2.9	3.1	3.2	3.5	3.1	3.5
14:10	2.5	4.4	4.2	4.1	3.9	4.1
14:20	3.7	5.5	5.4	5.1	4.8	5.2
14:30	4.8	6.7	6.9	6.7	6.5	7
14:40	6.3	7	6.8	6.6	6.8	7.5
14:50	6.4	6.3	6.1	6.4	6.2	6.0
15:00	6.1	6.2	6.2	6.1	6.3	6.8
15:10	6	5.8	5.7	5.5	5.2	5.8
15:20	5.5	4.8	5.5	5.5	4.9	5.6
15:30	5.7	4.9	5.5	5.5	5.1	5.7
15:40	4.5	4.4	5.2	5.3	5	5
15:50	4.5	4.5	5.2	5.1	4.8	4.8
16:00	4.7	5.2	6	5.8	5.5	5.6
16:10	5	4.5	4.9	5.2	5	5.3
16:20	4.3	4.6	5	5.7	5	5.3
16:30	4.5	5.1	5.8	5.7	5.2	5.5
16:40	5.1	4.8	5.5	5.6	5.4	5.7
16:50	4.6	5.2	5.4	5.8	5.6	6.5
17:00	5.4	5.2	5.6	5.6	5.5	5.8
17:10	5.1	5.2	5.4	5.3	5	5.2
17:20	4.6	4.3	4.5	4.7	4.5	4.5
17:30	4.2	3.8	4	4.3	4.2	4.4
17:40	3.8	3.7	3.9	4	3.9	4
17:50	3.5	3	3.4	3.7	3.4	3.4
18:00	2.9	4.3	4.9	4.9	4.8	4.9
18:10	3.4	4.5	5	4.8	4.6	4.9
18:20	4.6	4.4	4.9	4.7	4.6	4.8
18:30	4.2	4.2	4.7	4.4	4.4	4.7
18:40	4.1	3.8	4.4	4.2	4.1	4.5
18:50	3.9	3.4	3.7	3.7	3.5	4
19:00	3.5	2.1	2.2	2.7	2.2	2.9
19:10	2.5	2.9	3.5	3.6	3.6	3.8

19:20	2.7	2.8	3.4	3.7	3	3.4
19:30	2.9	2.9	3.3	3.8	3.1	3.4
19:40	3.1	3.1	3.2	3.5	3	3.4
19:50	3	2.6	2.4	2.6	2.4	2.8
20:00	2.7	1.8	2.2	2.3	2.1	2.4
20:10	2.4	1.7	2.1	2.5	1.9	2.1
20:20	2	2.2	2.4	2.8	2.4	2.7
20:30	2.1	1.7	2	2.3	2	2.2
20:40	2.3	3.7	4.1	2.9	2.1	1.6
20:50	2.2	3.7	4.1	4.2	3.2	2.1
21:00	4.5	3.8	3.7	3.7	3	2.3
21:10	3.6	3.5	3.3	3.5	3	2.4
21:20	3.7	3.6	3.1	3.4	2.9	2.5
21:30	3.4	3.2	3	3.2	2.7	1.9
21:40	3.2	3	2.9	3.2	2.8	2.3
21:50	3.1	4.3	4	3.9	3.9	2.4
22:00	4	4.4	4.7	4.6	4.2	2.8
22:10	4.5	5	5.4	5.4	5.2	4.8
22:20	4.4	5.2	5.4	5.5	5.6	4.4
22:30	5	6.1	6	5.8	5.5	4.7
22:40	5.8	5.5	5.5	5.3	5.3	5
22:50	5.8	5.6	6	5.6	5.7	5.5
23:00	5.4	6.6	6.8	6.3	6.5	6.3
23:10	6.3	6.6	6.8	6.5	6.6	6.6
23:20	6.6	6.2	6.3	5.8	6	5.9
23:30	6	5.7	5.6	5	4.8	4.7
23:40	5.7	6.1	5.8	4.7	4	3.8

Appendix 11: Instruments' Specifications

11.1: CDT-2000 HD Digital Tachometer operating specifications

Specifications

Resolution	.01 from 0 –100 .1 from 100 – 1,000 1 from 1000 – 99,999
Accuracy	± 0.02% of reading or ±1 digit
Display	5-Digit LCD, 10mm high
Decimal Point	Automatic
Memory System	Maximum, minimum, average and last reading (retained in memory for the life of batteries)
Measurement System	
Non-Contact	Visible LED light beam
Contact	Contact adapter
Engineering units	
RPM	RPM
Surface Speed	Feet/min, inches/min and meters/min
Length	Feet, inches, meters

Sensing Distance	Up to 24 inches (60 cm)
Display Update Time	0.5 seconds or one measuring period
Auto Power Off	After 30 seconds of non-use (minimum, maximum average, and last reading retained in memory)
Battery Life	40 hours continuous use (approx.) with alkaline batteries
Battery Type	2 AA (1.5 V) or rechargeable
Weight	6 ounces (170 grams)
Housing Material	ABS Plastic
Operating Temperature	32 to 122° F (0 to 50° C)
Storage Temperature	–4 to 158° F (–20 to 70° C)

Measuring Ranges – rpm

Optical	1 – 99,999 rpm
Mechanical	1 – 99,999 rpm

Measuring Ranges – speed

Wheel Size	6"	12"	0.1 m
m/min	0.10–1524	0.40–609.6	0.10–1999
ft/min	0.40–5000	0.40–2000	0.40–6550
in/min	4.0–60.00	4.00–24.000	4.00–78.700
m/sec	0.10–25.40	0.10–10.16	0.10–33.30
ft/sec	0.10–83.33	0.10–33.33	0.10–109

Measuring Ranges – length

0 – 99,999 m, / 0 – 99,999 ft / 0 – 99,999 in

1. **Units of Measure Indicators** show the user-selected units of measure.
2. **Contact Indicator** shows if contact or non-contact operation is selected.
3. **Low Battery Indicator** alerts the operator if the batteries are low.
4. **On-Target Indicator** confirms that the measurements are reliable.
5. **Memory Indicators** are illuminated when the maximum, minimum, average and last readings are recalled to the display for viewing.

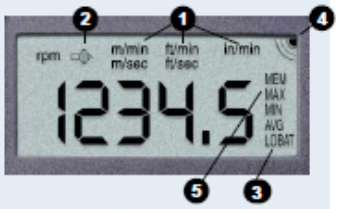

The CDT-2000HD is supplied as a complete kit including: Gauge, contact adapter, cone tip adapter, 6" circumference universal surface speed wheel, reflective tape, NIST-traceable calibration certificate, operating instructions and foam-fitted, hard-plastic carrying case.

A Non-Contact Model, the CDT-1000HD is also available.

CHECK•LINE® – PRECISION QUALITY CONTROL INSTRUMENTS

Electromatic Equipment Co., Inc.
600 Oakland Ave.
Cedarhurst, N Y 11516 —USA

Tel: (800) 645-4330 (USA & Canada)
Tel: (516) 295-4300
Fax: (516) 295-4399

Email: info@checkline.com
Website: www.checkline.com

FOR ADDITIONAL INFORMATION OR TO PLACE AN ORDER CALL TOLL FREE 1-800-645-4330

11.2: HD 300 Hand held Anemometer

EXTECH INSTRUMENTS
A FLIR COMPANY

Experience the Extech Advantage

PRODUCT DATASHEET

CFM/CMM Thermo-Anemometer with IR Temperature

Built-in IR Thermometer
Measures non-contact surface temperatures of objects unsafe or difficult to reach

Features:

- InfraRed Thermometer measures remote surface temperatures to 932°F (500°C) with 30:1 distance to spot ratio and Laser pointer
- Simultaneous display of Air Flow in CFM/CMM or Air Velocity plus Ambient Temperature
- Easy to set Area dimensions are stored in the meters internal memory for the next power on
- Large (9999 count) LCD backlit display
- 20 point average for air flow
- USB port includes software
- Includes Windows® compatible software with cable, vane sensor with 3.9ft (120cm) cable, hard carrying case, and 9V battery

BUILT IN IR Thermometer
Patented

Patented non-contact InfraRed Thermometer technology built into a Thermo-Anemometer is perfect for HVAC applications.

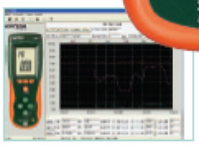

USB port includes PC Software

Specifications	Range	Accuracy
IR Temperature (non-contact)	-58 to 932°F (-50 to 500°C)	±2%
ft/min	80 to 5900 ft/min	±3%
m/s	0.4 to 30.00 m/s	±3%
km/h	1.4 to 108.0 km/h	±3%
MPH	0.9 to 67.0 MPH	±3%
knots	0.8 to 58.0 knots	±3%
Temperature	14 to 140°F (-10 to 60°C)	±4°F (2°C)
CFM/CMM	0 to 999900	
Dimensions	8x3x1.9" (203x75x50mm)	
Weight	9.8oz (280g)	

Ordering Information:

HD300 .....CFM/CMM Thermo-Anemometer with IR Temperature
HD300-NIST ..HD300 with Calibration Traceable to NIST.
TR100 .....Tripod

CE 3 YEAR WARRANTY

www.extech.com

9/19/11 - R1

11.3 C.A. 8333 Chauvin Arnoux Digital Power Analyser

Technical specifications

		C.A 8331	C.A 8333	C.A 8336	C.A 8435
Number of channels		3U / 4I		4U / 4I	
Number of inputs		4V / 3I		5V / 4I	
Voltage (TRMS AC+DC)		2 V to 1,000 V			
	Voltage ratio	up to 500 kV			
Current (TRMS AC+DC)	MN clamps	MN93: 500 mA to 200 Aac; MN93A: 0.005 Aac to 100 Aac			
	C193 clamp	1 A to 1,000 Aac			
	AmpFlex® or MA193 clamps	100 mA to 10,000 Aac			30 A to 6,500 Aac
	PAC93 clamp	1 A to 1,300 Aac/dc			
	E3N clamp	50 mA to 100 Aac/dc			
	Current ratio	up to 60 kA			
Frequency		40 Hz to 69 Hz			
Power values		W, VA, var, VAD, PF, DPF, cos φ, tan φ			
Energy values		Wh, varh, VAh, VADh			
Harmonics		yes			
	THD	yes, orders 0 to 50, phase			
	Expert mode	-	yes		
Transients		-	50	210	
Flicker	Pst	yes			
	Plt	-	-	Yes	
Inrush mode		-	yes on 4 periods	yes > 10 minutes	
Unbalance yes		yes			
Recording	Min/Max	yes			
	of a selection of parameters at the max. sampling rate	4 hours to 2 weeks	A few days to several weeks	2 weeks to several years	
Alarms		-	4,000 of 10 different types	10,000 of 40 different types	
Peak		yes			
Vectorial representation		automatic			
Display		Colour ¼ VGA TFT screen, 320 x 240, diagonal 148 mm			
Capture of screens and curves		12		50	
Electrical safety		IEC 61010 1,000 V CAT III / 600 V CAT IV			
Protection		IP53 / IK08			IP67
Languages		more than 27			
Communication interface		USB			
Battery life		up to 13 hours			
Power supply		9.6 V NiMH rechargeable battery or external mains charger			
Dimensions		240 x 180 x 55 mm			270 x 250 x 180 mm
Weight		1.9 kg			3.7 kg

STATE AT DELIVERY FOR THE C.A 8336, C.A 8333 AND C.A 8331

Models without sensors

One Qualistar+ analyser delivered with a bag for accessories, 5 x 4 mm banana voltage leads 3 m long, 5 crocodile clips, a set of 12-colour inserts/rings for identifying the leads and inputs, a scratch-proof screen-protection film (mounted), a USB cable, a mains power cable, a mains power pack, a safety datasheet, a multi-language operating manual CD and a PC data retrieval software CD (Power Analyser Transfer).

STATE AT DELIVERY FOR THE C.A 8435

C.A 8435 AMP450: delivered with bag no. 22, USB cable, IP67 mains power cable, 4 AmpFlex® 450 IP67 A196 current sensors, 5 x 3 m black IP67 BB196 banana leads, 5 lockable crocodile clips, 12-colour identification kit for the leads and inputs, scratchproof screen-protection film (mounted), safety datasheet, CD containing the multi-language operating manual and CD PC data retrieval software and CD containing PC data retrieval software (Power Analyzer Transfer).

References for ordering

C.A 8336 alone	P01160591
C.A 8333 alone	P01160541
C.A 8331 alone	P01160511
C.A 8435 alone	P01160585
C.A 8435 AmpFlex® 450 mm	P01160587

Accessories and replacement parts

MN93 clamp	P01120258	Qualistar screen film	P01102059
MN93A clamp	P01120348	Set of id. rings/inserts	P01102080
MiniFlex® MA193, 250 mm	P01120580	Set of caps (C.A 8435)	P01102117
MiniFlex® MA193, 350 mm	P01120567	Set of 5 x 3 m IP67 (BB196) banana leads	P01295479
PAC93 clamp	P01120798	Carrying bag no. 21	P01298055
AmpFlex® A193 450 mm clamp	P01120268	Carrying bag no. 22	P01298056
AmpFlex® A193 800 mm clamp	P01120318	USB-A USB-B lead	P01295293
AmpFlex® A196 450 mm IP67 clamp	P01120552	5 A box	P01101959
C193 clamp	P01120238	Mains power pack (C.A 8331-33-35-36)	P01102057
E3N clamp	P01120043A	IP67 mains lead (C.A 8435)	P01295477
E3N Adapter	P01102081	Dataview® Software	P01102095
E3N mains power pack	P01120047	Lockable crocodile clips (x 5)	P01102099
J93 clamp	P01120110	Kit containing 5 banana leads, 5 crocodile clips and 1 set of coloured rings	P01295483
Battery pack	P01296024	Kit containing 4 banana leads, 4 crocodile clips and 1 set of coloured rings	P01295476
ESSAILEC casing	P01102131		
Reeling Box	P01102149		
PA31ER mains adapter	P01102150		

CHAUVIN ARNOUX GROUP

FRANCE
Chauvin Arnoux
190, rue Championnet
75876 PARIS Cedex 18
Tel: +33 1 44 85 44 38
Fax: +33 1 46 27 95 59
export@chauvin-arnoux.fr
www.chauvin-arnoux.com

UNITED KINGDOM
Chauvin Arnoux LTD
Unit 1 Nelson Ct, Flagship Sq, Shaw Cross Business Pk
Dewsbury, West Yorkshire - WF12 7TH
Tel: +44 1924 460 494
Fax: +44 1924 455 328
info@chauvin-arnoux.co.uk
www.chauvin-arnoux.com

MIDDLE EAST
Chauvin Arnoux Middle East
P.O. BOX 60-154
1241 2020 JAL EL DIB - LEBANON
Tel: +961 1 890 425
Fax: +961 1 890 424
camie@chauvin-arnoux.com
www.chauvin-arnoux.com

For assistance and ordering

11.4 Fluke P.M. 3384a Digital Oscilloscope

Technical Specifications

ANALOG MODE

VERTICAL DEFLECTION

Input channels
Full attenuator control on all four input channels (PM 33x4B), or on both input channels (PM 33x0B). External trigger input signal can be displayed for "trigger view" (PM 33x0B). On screen channel identifiers with ground level indicator.

Display modes
PM 33x4B: CH1, +/- CH2, CH3, +/- CH4, Add, Subtract; Alternate or chopped automatically selected.

PM 33x0B: CH1, +/- CH2, Add, Subtract; External Trigger View; Alternate or chopped automatically selected.

Bandwidth (+5.... +40°C)
PM 339xB: >200 MHz @ -3 dB,
PM 338xB: >100 MHz @ -3 dB,
PM 3370B: > 60 MHz @ -3 dB.

Bandwidth limiter
20 MHz @ -3 dB on all fully controllable channels simultaneously.

Rise time
(calculated from the bandwidth)
PM 339xB: < 1.75 ns,
PM 338xB: < 3.5 ns,
PM 3370B: < 5.8 ns.

Deflection Settings
Step attenuator:
2 mV/div..... 5V/div. in a 1-2-5 sequence (full bandwidth).
Calibrated vernier:
2 mV/div.... 12.5 V/div.

External Trigger View (PM 33x0B):
100 mV/div. and 1 V/div.

Error limits
1.3% (measured over central 6 divisions).

Input impedance
All models, all channels:
1 MΩ ± 1% // 25 pF ± 2 pF
PM 339xB: user selectable 50Ω ± 1%.

Max. rated input voltage
In 1 MΩ position: ±150 V_{rms} CAT II
In 50Ω position: dc:±5 V, rms: 5 V, ACpeak:±50 V.

Dynamic range
PM 339xB: 24 div. at 50 MHz
PM 338xB: 24 div. at 25 MHz
PM 3370B: 24 div. at 15 MHz

CMRR
100:1 at 1 MHz, 25:1 at 50 MHz.

Channel isolation
PM 339xB: 50:1 at 200 MHz
PM 338xB: 50:1 at 100 MHz
PM 3370B: 50:1 at 60 MHz

HORIZONTAL
(Main and Delayed Timebase)

Display modes
Main Timebase (MTB),
Delayed Timebase (DTB),
Alternate Timebase (= MTB and DTB),
X-Y mode.

Sweep speeds (magn. x1)
PM 339xB: MTB: 0.5 s/div..... 20 ns/div. in a 1-2-5-sequence. Calibrated vernier gives 1.25 s/div..... 20 ns/div. DTB: 0.5 ms/div... 20 ns/div. in a 1-2-5 sequence.
PM 338xB and PM 3370B: MTB : 0.5 s/div.... 50 ns/div. in a 1-2-5-sequence. Calibrated vernier gives 1.25 s/div ..... 50 ns/div. DTB: 0.5 ms/div... 50 ns/div. in a 1-2-5-sequence.

Fastest sweep speed (magn. x10)
PM 339xB: 2 ns/div.
PM 338xB and PM 3370B: 5 ns/div.

Error limit (magn. x1)
≤ [1.3% of reading + 0.5% of 8 divisions].

DELAY TIME MULTIPLIER

Resolution
1 : 40,000

Error limit (magn. x1)
≤ [0.8% of reading + 0.3% of 8 divisions + 4 ns].

Jitter
< 1 : 25,000

TRIGGERING
(Main and Delayed timebase)

Trigger modes
Auto free run, Triggered, Single;
Edge triggering, TV Triggering.

EDGE TRIGGERING

MTB trigger source
PM 33x4B: CH1.... CH4, Line. External trigger input optional, replacing "Line".
PM 33x0B: CH1, CH2, External, Line.

DTB trigger source
Starts after delay or triggered on any channel or on External Trigger input (PM 33x0B only).

Slope
Positive (+), Negative (-).

Coupling
DC, AC (<10 Hz), LF-rej. (30 kHz), HF-rej. (30 kHz).

Trigger gap
0.4 div., user selectable 0.8 div. for triggering on noisy signals.

Level range
± 8 div. or automatically within signal peak-peak amplitude range.

Level indication
On screen level indicators and numerical read-out.

Trigger sensitivity and bandwidth
(+5.... +40°C)

Sensitivity	PM339xB	PM338xB	PM3370B
0.6 div.	30 MHz	50 MHz	100 MHz
1.2 div.	60 MHz	100 MHz	200 MHz
2.0 div.	150 MHz	200 MHz	300 MHz

TV Triggering

MTB trigger source
PM 33x4B: CH1.... CH4; Lines, Field 1, Field 2, specific line using built-in line counter. External trigger input optional, replacing "Line"
PM 33x0B: CH1, CH2, Ext.; Lines, Field 1, Field 2, specific line using built-in line counter.

Video standard
NTSC, PAL, SECAM, HDTV.

Delayed TB trigger source
Starts after delay or triggered on any input channel or on External Trigger input (PM 33x0B only); DTB triggers on edge or on TV line. The Delayed TB can be used to expand any part of the line selected with the video line selector.

Signal polarity
Positive or negative video.

Sensitivity
0.7 div. (amplitude of sync. pulse).

X-Y MODE

X-deflection source
PM 33x4B: CH1.... CH4, Line.
PM 33x0B: CH1, CH2, External, Line.

X-deflection coefficient
Same as for vertical deflection, error limit 5% over central 6 div.

Dynamic range
20 div. up to 100 kHz,
> 10 div. up to 2 MHz.

ANALOG MODE (cont.)

Frequency response
≥ 2 MHz @ -3 dB.
Phase shift < 3° up to 100 kHz.

CURSOR MEASUREMENTS

Cursor modes and Read-out
Vertical: dV, V1 to ground, V2 to ground, ratio.
Horizontal: dT, 1/dT (in Hz), ratio, phase.
Horizontal and vertical cursors can be used together.

Accuracy (magn. x1)
± 1% of full scale within the central 8 horizontal and 6 vertical divisions.

DIGITAL MODE

ACQUISITION

Repetitive Sample Rate
Random sampling gives an equivalent sample rate up to 25 GS/s (PM 339xB) or up to 10 GS/s (PM 3370B and PM 338xB) on all input channels, over the full bandwidth.

Single Shot Sample Rate
Real time sampling up to 200 MS/s (single channel), 100 MS/s (dual channel).
In PM 33x4B, a fast chopper offers 200 ns horizontal resolution in 4 channel single shot mode.

Bandwidth (+5..... +40°C)
PM 339xB: 200 MHz (repetitive and single shot)
PM 338xB: 100 MHz (repetitive and single shot)
PM 3370B: 60 MHz (repetitive and single shot)

Calculated Maximum Captured Frequency in single shot mode
- Using sine interpolation to reconstruct signals at 5 samples per period:
  40 MHz in 1 channel mode,
  20 MHz in 2 channel mode,
  1 MHz in 4 channel mode or when trigger view (PM 33x0B) is active.
- For 10 samples per period with linear interpolation:
  20 MHz in 1 channel mode,
  10 MHz in 2 channel mode,
  0.5 MHz in 4 channel mode or when trigger view (PM 33x0B) is active.

ADC Resolution
ADC resolution 8 bit, Memory resolution 16 bit. All mathematical operations and averaging increase waveform resolution beyond 8 bits.

Memory
Memory resolution 16 bit; Acquisition and reference memory can be segmented offering the choice between long acquisition records or a maximum screen update rate and a maximum number of traces in memory. See table for full details on acquisition length selections and total number of traces that can be stored in back-up memory. Figures include the MTB acquisition memory as well as DTB acquisition memory (available with 512 samples acquisition length only).

Record length and trace storage

PM 3394B, PM 3384B				
Acquisition length	1 CH x 32K	2 CH x 16K	4 CH x 8K	4 CH x 512s
Trace storage	3 traces	6 traces	12 traces	208 traces
PM 3370B, PM 3380B and PM 3390B with Standard memory				
Acquisition length	1 CH x 8K	2 CH x 4K	2 CH + TrView x 2K	2 CH + TrView x 512s
Trace storage	3 traces	6 traces	9 traces	30 traces
PM 3370B, PM 3380B and PM 3390B with Expanded Memory option				
Acquisition length	1 CH x 32K	2 CH x 16K	2 CH + TrView x 8K	2 CH + TrView x 512s
Trace storage	3 traces	6 traces	9 traces	156 traces

Averaging
Averaging reduces random noise contained in the signal, while increasing the vertical resolution. Averaging factor user selectable: 2, 4, 8, ... 4096; Max. resolution: 14 bit.

Peak detection
Captures glitches as narrow as 5 ns at any timebase setting (single channel) or 10 ns (dual channel and multiple channel, alternating) and at correct amplitude. Also very useful to capture high-frequency components (like a modulated carrier) at low timebase settings.

Envelope mode
For continuous tracking of changing waveforms.

VERTICAL

Same as analog mode, unless specified otherwise.

Auto-ranging vertical deflection
Automatically and continuously adapts vertical deflection setting to have 2..... 6.4 division display of input signal. Can be selected on any input channel individually. Minimum deflection setting automatically selected is 50 mV/div.

Vertical Magnification
Up to 32x magnification for higher deflection sensitivity; can be combined with averaging for increased resolution (averaging factor selectable up to 4096x resulting in a vertical resolution of 14 bit).

Display modes
PM 33x4B: CH1, +/- CH2, CH3, +/- CH4; Calculated Add and Subtract.
PM 33x0B: CH1, +/- CH2; Calculated Add and Subtract. External Trigger Input signal can be displayed acting as a third input channel.

Bandwidth limiter
20 MHz @ -3 dB.

Window mode
2 or 4 windows to display two or four traces above each other while using the full dynamic range of the ADC (8 bit).

HORIZONTAL

Acquisition modes
Recurrent (Auto and Triggered), Single Shot, Multiple single shot (as part of Math+ option), Roll, Triggered Roll. User selectable AUTO-RANGING timebase in recurrent modes.

X-Y mode
X-source: any trace in memory or any of the input channels.

AUTO-RANGING timebase
Continuously adapts sweep speed to the frequency of the trigger signal in order to keep 2..... 6 cycles on screen; User selectable function. Autoranging Timebase can work with timebase in 1-2-5 range or with continuously variable timebase, stabilizing the number of cycles on screen.

Timebase modes
Main TB (MTB), Delayed TB (DTB), Alternate TB (= MTB and DTB).
Delayed timebase starts after delay or triggered on channel. Trigger coupling: same as for analog mode.

Timebase (magn. x1)
Real time sampling: 200 s/div.... 500 ns/div., 250 ns/div.
Recurrent: 200 ns/div..... 2 ns/div. (5 ns/div. for PM 338xB and PM 3370B)
Roll mode: 200 s/div..... 50 ms/div.

Variable timebase
Continuously variable sweep speed: 1 µs/div.... 500 ms/div. in 1 µs increments; 500 ms/div.... 200s/div. better than 0.2% increments.

Display resolution
Horizontal resolution (per trace) for x1 magnification: 500 samples = 10 divisions = 1 screen width. Compression allows a compact display of larger records.

DIGITAL MODE (cont.)

Magnification
x2, x4, ... x32 (expansion) of any part of a record;
x1/2, x1/4, ... x1/64 (compression) of records exceeding 512 samples.

Interpolation
- Dots only (shows acquired samples only).
- Linear interpolation.
- Sine interpolation (offers natural representation of expanded single shot acquisitions up to <10 ns/div.).

TRIGGERING

Edge triggering
Same as for analog mode, plus dual slope triggering when used in single shot, real time only mode.

TV triggering
Same as for analog mode.

Logic triggering modes
State (4 bit), Pattern (4 bit), Glitch (time qualified pulse).
- **State triggering** (PM 33x4B only)
  Any of the 4 channels can be selected as the clock. Each of the other channels can be monitored for being "high", "low" or "don't care". The scope triggers if the combination of the remaining channels matches the user defined description during a transition (+ or –, user selectable) of the clock.
  Max. clock rate: 150 MHz typical.
  Sensitivity: 1.0 div. if time present ≥ 10 ns (≥ 20 ns for PM 3384B), 2 div. if time present ≥ 2 ns (≥ 4 ns for PM 3384B).
- **Pattern triggering** (PM 33x4B only)
  The scope triggers if the combination of the four channels matches the user defined description. Each channel can be monitored for being "high", "low" or "don't care".
  Modes: Enter, Exit, Time qualified (lower limit, upper limit, range).
  Range of limits: 20 ns.... 167.7 ms;
  Smallest resolution: 10 ns;
  Sensitivity: 1.0 div. if time present ≥ 10 ns, (≥ 20 ns for PM 3384B), 2 div. if time present ≥ 2 ns, (≥ 4 ns for PM 3384B).
- **Glitch triggering** (all models)
  Minimum glitch width:
  2 ns (4 ns PM 339xB), 4 ns (PM 338xB) or 6 ns (PM 3370B).
  Pulse width time qualification:
  lower limit, upper limit, range.
  Limits must be in the range 20 ns... 167.7 ms; Smallest resolution 10 ns.

DELAY

Time delay
0.... 1000 div., continuously adjustable.
Pre-trigger view
Up to 1 full record (= 160 div. for an 8K record, or 640 div. for a 32K memory)

Event delay
1.... 16384 events;
Max. count rate 50 MHz (typical);
Source: any channel (including External Trigger on PM 33x0B); Modes: Event delay, Time delay after event delay.

Delay modes
Start after time delay, Wait for trigger after time delay.

CURSOR MEASUREMENTS

Cursor modes
Horizontal, Vertical, Both; Free or coupled to trace. Cursors can be used throughout the memory.

Read-out

Vertical:	dV, V1 to ground, V2 to ground, dVratio
Horizontal:	dT, 1/dT (in Hz), T1&T2 to trigger moment, dTratio, phase.

For phase measurements, the cycle is automatically referenced to trigger signal.

CALCULATED MEASUREMENTS

General
Measurements can be performed over a complete record or within a cursor limited area. Statistics mode provides minimum, mean and maximum measurement result per measurement.

Volt
DC, RMS, Minimum, Maximum, Peak to Peak, Low level, High level, Overshoot (pos. or neg.), Preshoot (pos. or neg.).

Time
Frequency, Period, Pulsewidth, Rise time, Fall time, Duty cycle.

Delay
Between channels; Rising and falling edges independently selectable.

Quick Measurement
Probe mounted "Command Switch" operates "Touch, Hold and Measure', giving calculated measurements of frequency, V_{DC}, V_{RMS} and V_{pp}.

PROCESSING

Standard
Add, Subtract, Multiply, Digital filter (for noise reduction and increased resolution by means of digital low pass filtering after single shot capture).

In Math+ option
Integrate, Differentiate, FFT, Histogram.

GENERAL

INTERFACING

RS-232C SERIAL INTERFACE

Interface installed as a standard. Enables printing and plotting as well as full remote control of the instruments. Also allows for serial communication trace dump to arbitrary waveform generator.
DB-9 male connector.

Handshake
DSR/DTR, CTS/RTS, or Xon/Xoff.

Baudrate
75.... 19k2 full duplex, 38k4 dump only.

Format
1 stopbit; 7 or 8 databits; odd/even/no parity.

Protocol
CPL = Compact Programming Language; A reduced set of powerful instruction for full remote control through RS-232C.

Waveform dump
Trace dump to PM 5150, PM 5138A and PM 5139 arbitrary waveform generator (requires generator to be equipped with RS-232C interface).

GPIB/IEEE-488.2 INTERFACE

Factory installed option (next to RS-232C). Remote control conform SCPI (Standard Commands for Programmable Instruments) = standardized protocol. Fully compatible with IEEE-488.2.

Waveform dump
Trace dump to PM 5150, PM 5138A and PM5139 arbitrary waveform generator (requires generator to be equipped with IEEE interface).

HARDCOPY

Using RS-232C (standard) or GPIB/IEEE-488.2 (optional) interface. Centronics output optionally available through PAC33 Print Adapter Cable, giving RS-232 to Centronics conversion.

Output
Printed or plotted hardcopy of the screen (digital mode) in sizable format. If selected, with status report of the complete instrument setting and date- and timestamp of the trigger moment and the moment the hardcopy action was started. Two lines of on-screen text (32 characters per line) can be added for user documentation.

Printers
9 pin matrix printers (FX-80 compatible), 24 pin matrix printers (LQ-1500 compatible), ThinkJet (HP2225) and compatibles, HP LaserJet (series II & III) and compatibles incl. HP DeskJet, HP540 DeskJet compatibles.

Plotters
HP7440, HP7470A, HP7475A, HP7550, standard HPGL, PM8277, PM8278 and compatibles. HPGL file format is recognized by most drawing- and wordprocessor packages for direct inclusion of screen plots in documents, reports etc.